INSTITUTE FOR RESEARCH, INC.
8330 WESTGLEN DR. • HOUSTON, TEXAS 77042 • 713/783-8400

CR-134204

FINAL REPORT

DEVELOPMENT OF CONCEPT FOR CONCURRENT BIOCIDE GENERATION AND WATER SYSTEM PURIFICATION

Contract NAS 9-12998

Exhibit "A"

Development of Concept for Concurrent Biocide Generation and Water System Purification

The general objectives of this work are outlined as follows:

1. Measure iodine production rates as a function of potential to determine optimum potentials.

2. Measure iodine production rates as a function of iodine concentration to determine the lower limit of iodide concentration that can be used.

3. Study the effect of electrode size and geometry upon iodine production rates.

4. Study the feasibility of using stainless steel as reference electrodes.

5. Compare polarization curves of stainless steel in corrosive sulphuric acid to those in dilute solutions of KI.

6. Construct and demonstrate a scaled laboratory model of the proposed electrochemical system.

Background

Our previous work showed that larger and more reproducible iodine production rates were obtained in a cell in which the cathode and anode were separated by a glass frit. This arrangement prevented iodine generated at the anode from being reduced at the cathode. Unless otherwise noted, all work presented was done in a two compartment cell as illustrated in Figure 1A. The potentiostatic circuit for maintaining constant potentials is illustrated in Figure 1B.

A small amount of stirring increased anodic currents which at -1150 mv represented increasing iodine production rates. Stirring was accomplished by a magnetic stirring bar and a variable rheostat. The voltage output from the rheostat was used as a measure of the stirring or convection rate. Below a setting of eight volts the stirrer did not move. As illustrated in Figure 2, increasing the voltage from 10v to 100v appeared to increase the anodic current, but upon decreasing the voltage from 100v to 10v, the current remained sensibly constant at 1.28 ma. At a pre-set voltage, the current slowly increased to approximately 1.28 ma. Since it was observed that a small amount of stirring increased

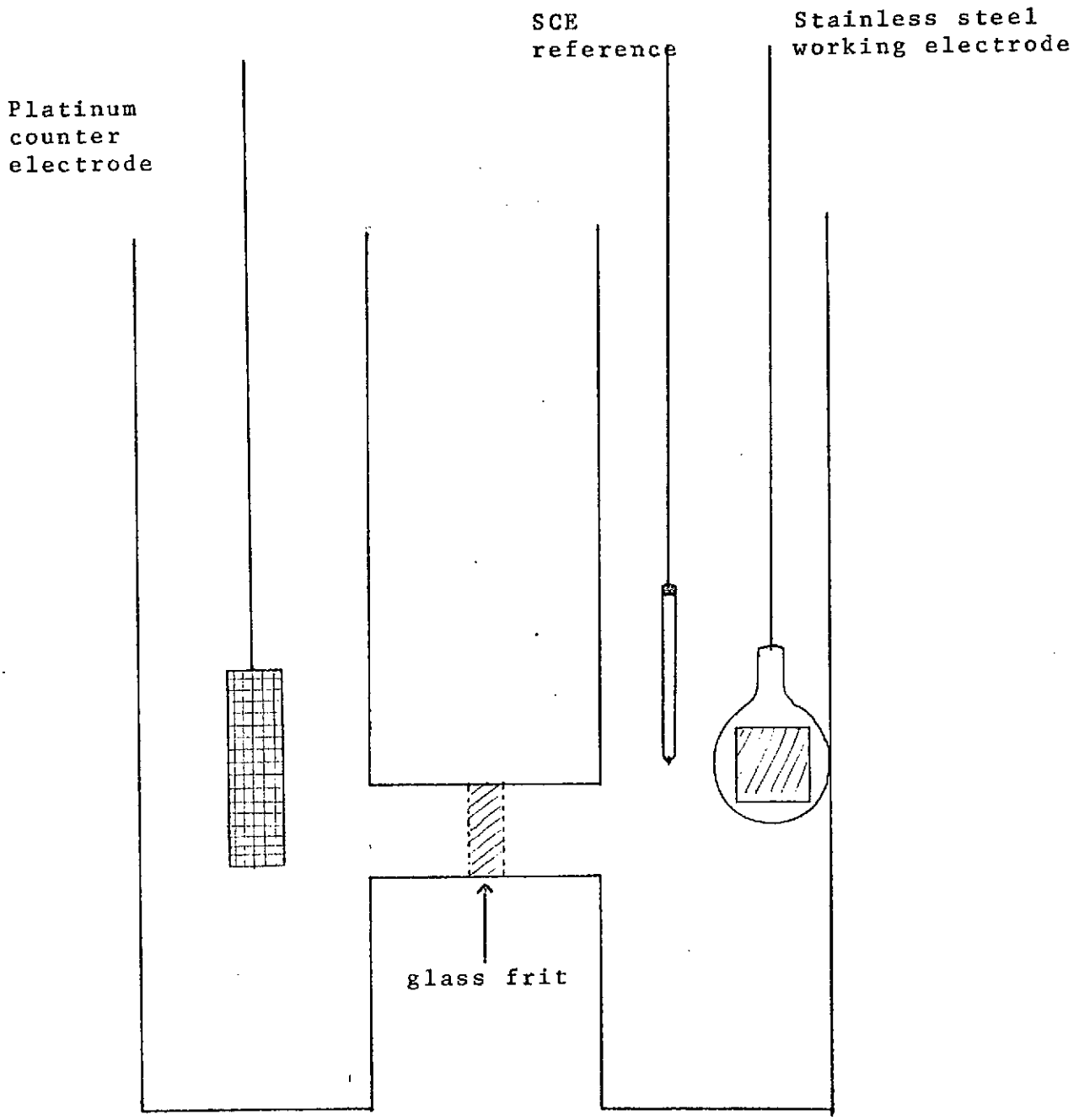

Figure 1A. Schematic of Electrochemical Cell

Figure 1B

Schematic Diagram of the Circuit Used
to Maintain a Constant Potential

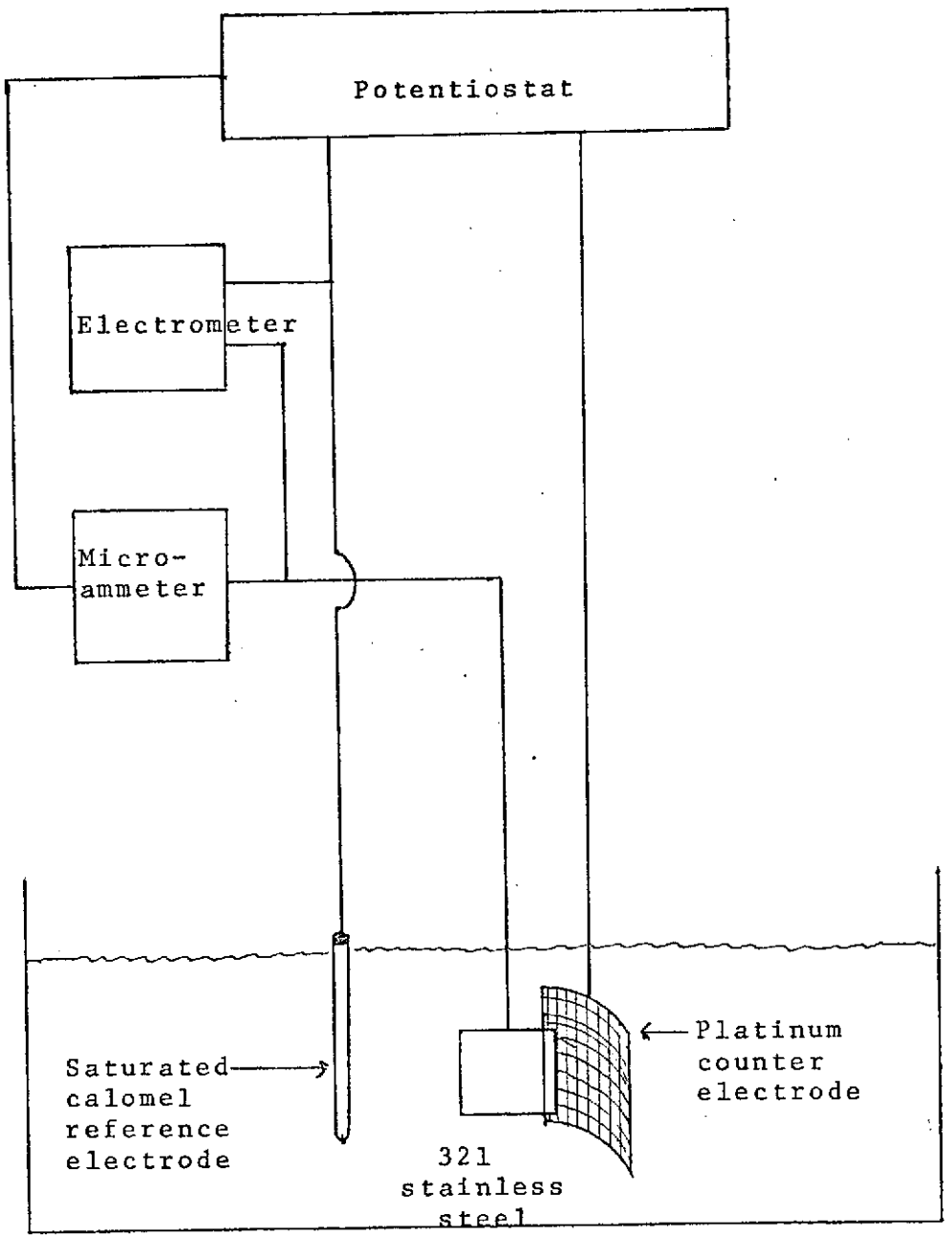
Potentiostat
Electrometer
Micro-
ammeter
Saturated
calomel
reference
electrode
321
stainless
steel
Platinum
counter
electrode

Fig. 1B

iodine production rates as much as higher voltages, a setting of 10v was arbitrarily selected to represent a constant stirring rate.

Iodine concentrations, as measured with the Beckman iodine meter, did not increase linearly with time, particularly at longer time periods. Since the iodide solutions used were relatively dilute (maximum of 382 ppm I^-), the iodide concentration decreased significantly with time during the experiment. When iodine concentrations were calculated on the basis of continuing source of iodide to maintain the initial iodide concentration, the iodine concentration-time relationship became linear. The calculations were based on the following empirical formula:

$$[\text{iodine}]_{\text{projected}} = [\text{iodine}]_{\text{measured}} \left(\frac{[I^-]_{\text{initial}}}{([I^-]_{\text{initial}} - n[\text{iodine}]_{\text{measured}})} \right)$$

where n is 2 for the reaction $2I^- \rightarrow I_2 + 2e$, and n is 3 for the reaction $3I^- \rightarrow I_3^- + 2e$. The data presented in this report are projected iodine concentrations and rates of evolution.

Initially the potentials, currents, and iodine production rates were not stable and reproducible. The main reason for instability of these measurements was the non-equilibrium state of the working electrode. Table I. and Figure 3. shows

the initial iodine production rates. Initially some difficulty was also encountered in maintaining potentials more anodic than 900 mv vs. SEC. When the electrochemical cell was surrounded by aluminum foil (Faradaic cage) and electrically connected to water pipe ground, potentials, currents and iodine production rates became more stable and reproducible. The electrochemical cell was electrically grounded in all expreiments following these initial observations and measurements.

The Beckman iodine meter measures only I_2 concentrations and in the presence of iodide, I_2 usually exists as the triiodide ion (ie,I_3^-). For comparison purposes iodine concentrations and rates assume both species in this report.

Figure 2.

Effect of stirring on current for 321 Stainless Steel in a 500 ppm KI (382 ppm I^-) solution at +1150 mv vs. SCE

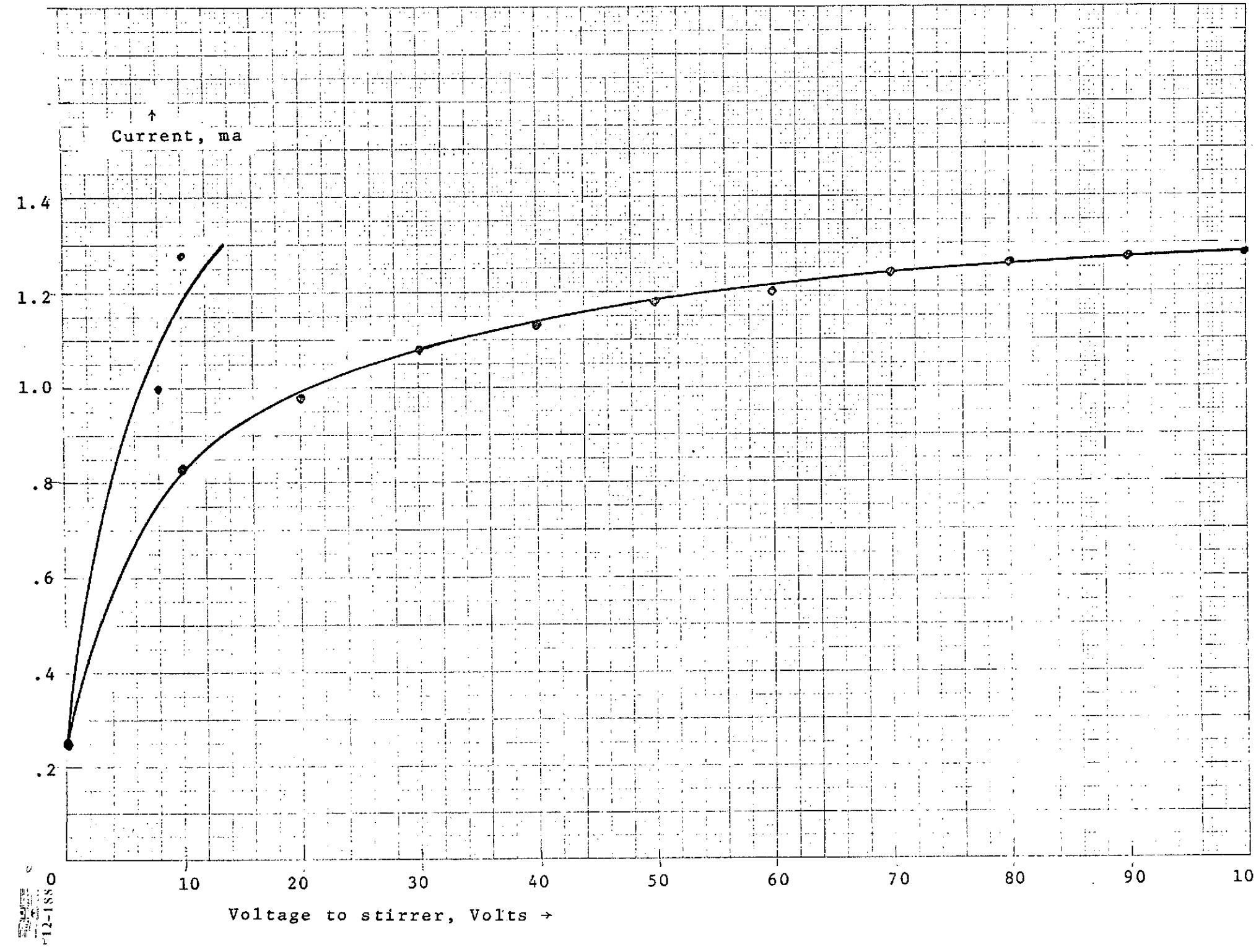

Fig. 2.

12-188

10 Millimeters to the Centimeter

Figure 3.

Effect of anodic polarization upon iodine production rates. 500 ppm KI (382 ppm I-) in distilled water. Stirrer set at 10 volts. Surface area = 0.54 cm^2. Anode was 321 Stainless Steel. The electrochemical cell was not electrically grounded. Room conditions. Iodine concentrations are based on 382 ppm I^- constantly present and on the reaction $3I^- \rightarrow I_3^- + 2e$.

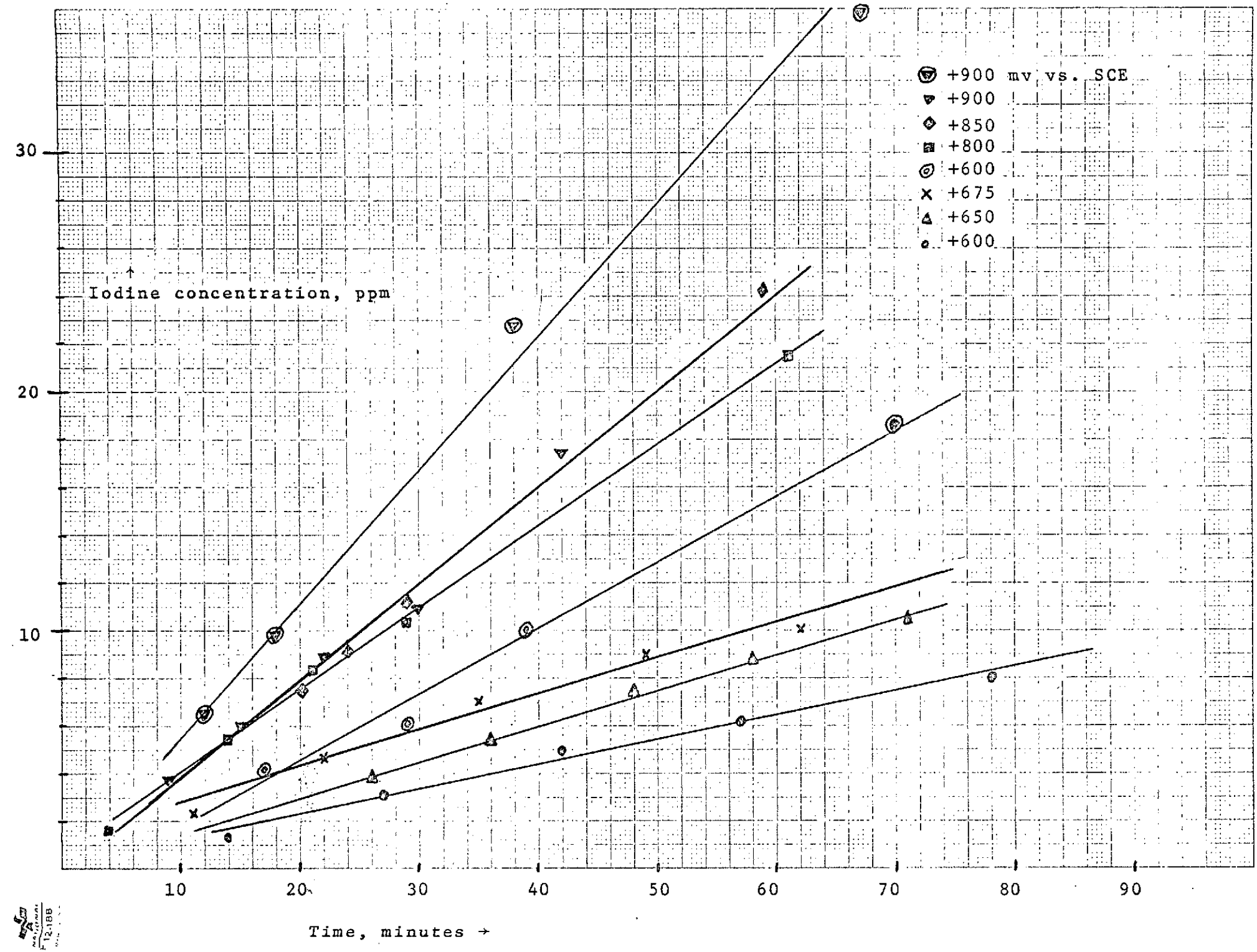

Fig. 3

10 Millimeters to the Centimeter

TABLE I.

Iodine production rates at anodic potentials shown in Figure 1.

Potential (mv vs. SCE)	Iodine Production Rate (ppm/minute)
+900	0.56
+900	0.40
+850	0.40
+800	0.34
+600	0.27
+675	0.16
+650	0.15
+600	0.10

Iodine Production Rates

The iodine concentration-time relationship under constant anodic polarization are shown in Figures 4A, 4B, 5A, and 5B. Iodine production rates at these applied potentials are listed in Table II. The rate of iodine production was observed to increase in the anodic region of +750 mv to +1150 mv vs. SCE. In the region of potential of +1150 and +1500 mv, the rates became essentially constant. This is shown more clearly in Figure 5 in which the iodine production rate-constant potential relationship is plotted on the same graph and compared with iodine production rates calculated from a typical potentiostatic polarization curve.

Up to +1000 mv the measured and calculated iodine rates for both I_2 and I_3^- are in good agreement and within acceptable experimental error limits. At potentials more anodic than +100 mv, the iodine rates calculated from the polarization curve are larger than those measured. This difference appears even larger because the measured iodine rates are projected on the basis of a constant iodide concentration. These larger currents may be due to oxidation of iodine (either I_2 or I_3^-) to a hydrated iodine species as

Figure 4.

A. Assuming the reaction $2I^- \rightarrow I_2 + 2e$

B. Assuming the reaction $3I^- \rightarrow I_3^- + 2e$

Increase of iodine concentrations with time on 321 Stainless Steel under constant anodic polarization. Surface area was 0.54 cm^2. Room conditions.

A. Values based on 382 ppm I^- assuming the reaction $2I^- \rightarrow I_2 + 2e$

B. Values based on 382 ppm I^- assuming the reaction $3I^- \rightarrow I_3^- + 2e$

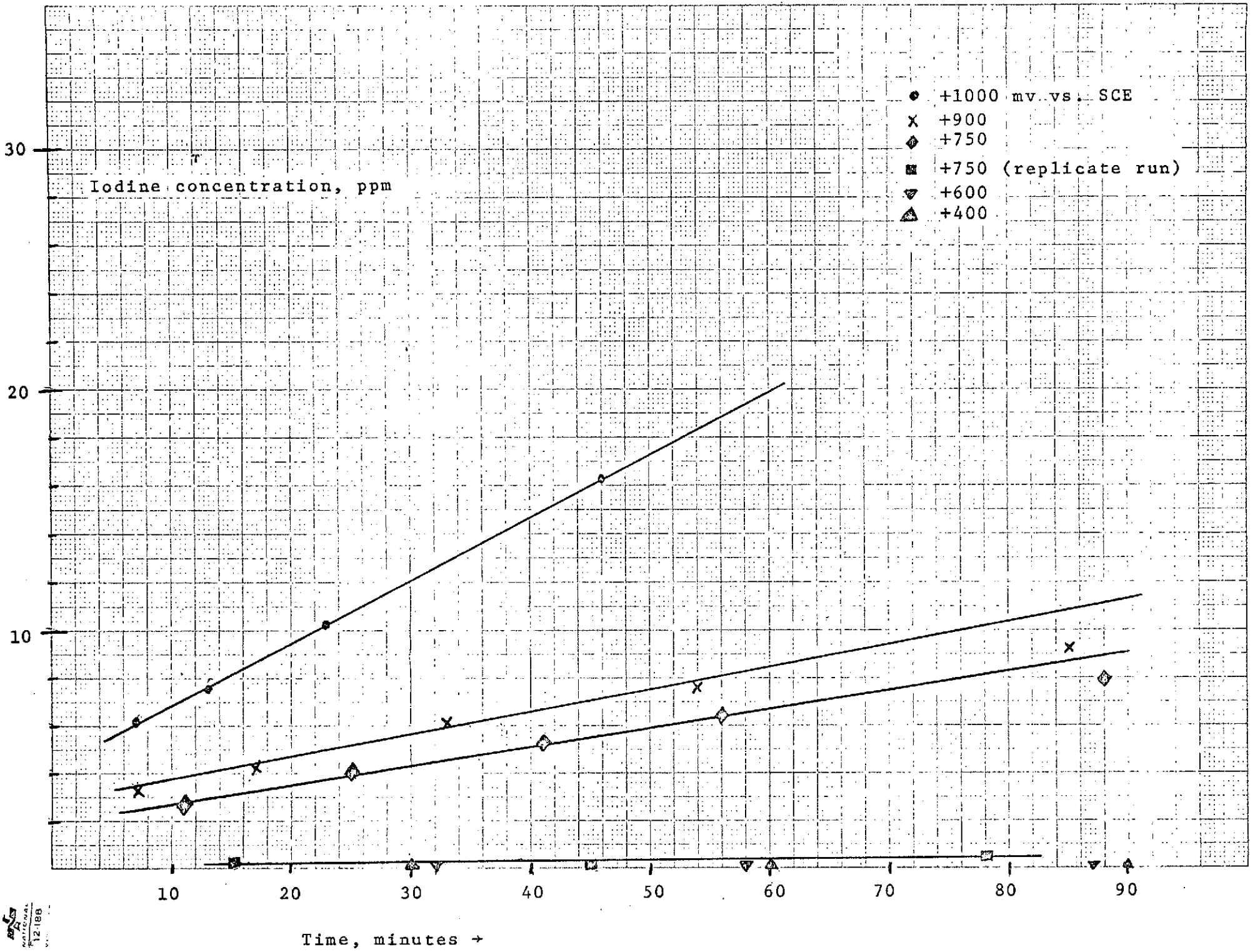

B

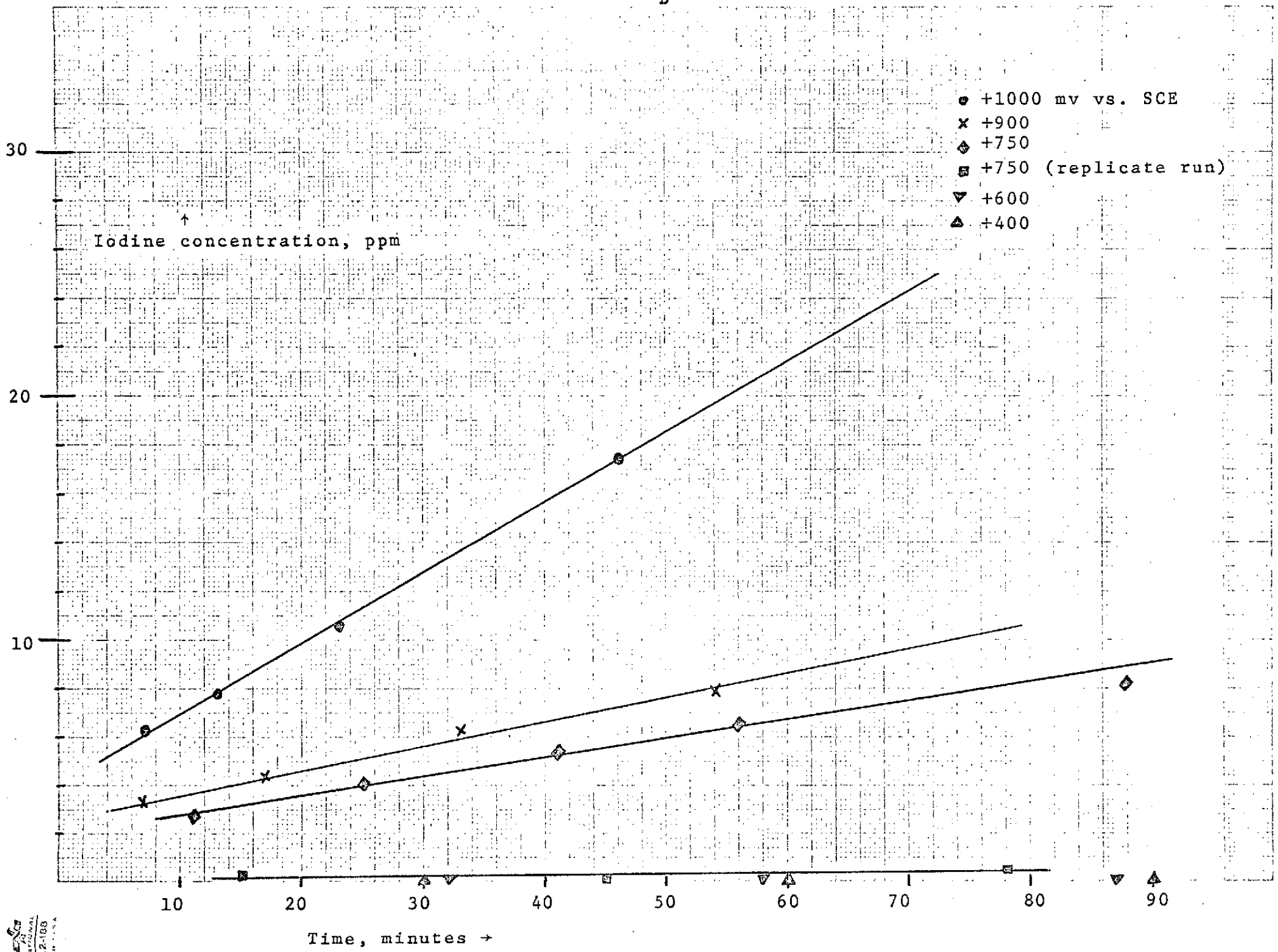

Figure 5.

Effect of larger anodic polarizations upon the iodine concentration-time relationships.

A. Assuming the reaction $2I^- \rightarrow I_2 + 2e$

B. Assuming the reaction $3I^- \rightarrow I_3^- + 2e$

A.

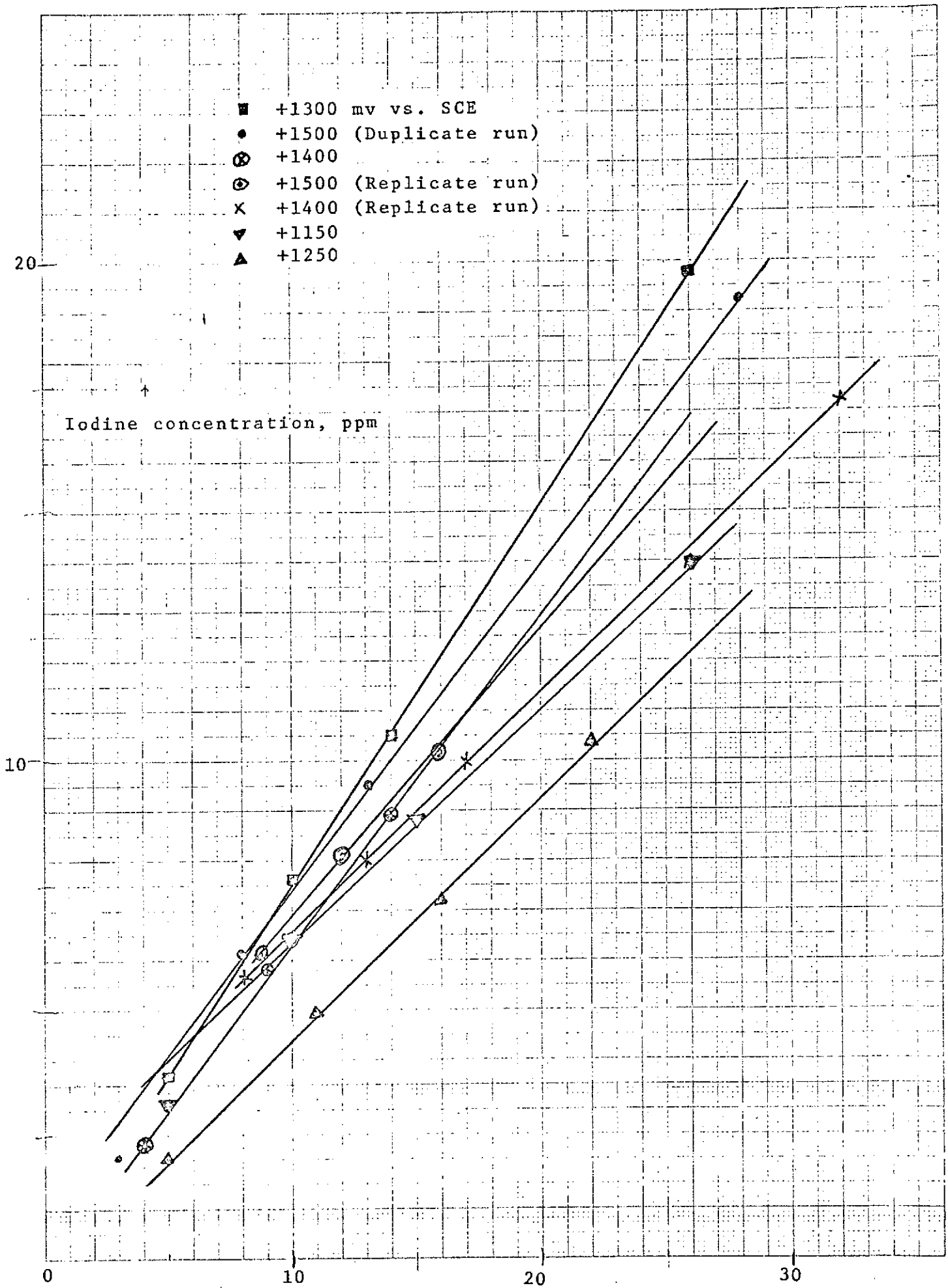

10 Millimeters to the Centimeter

B.

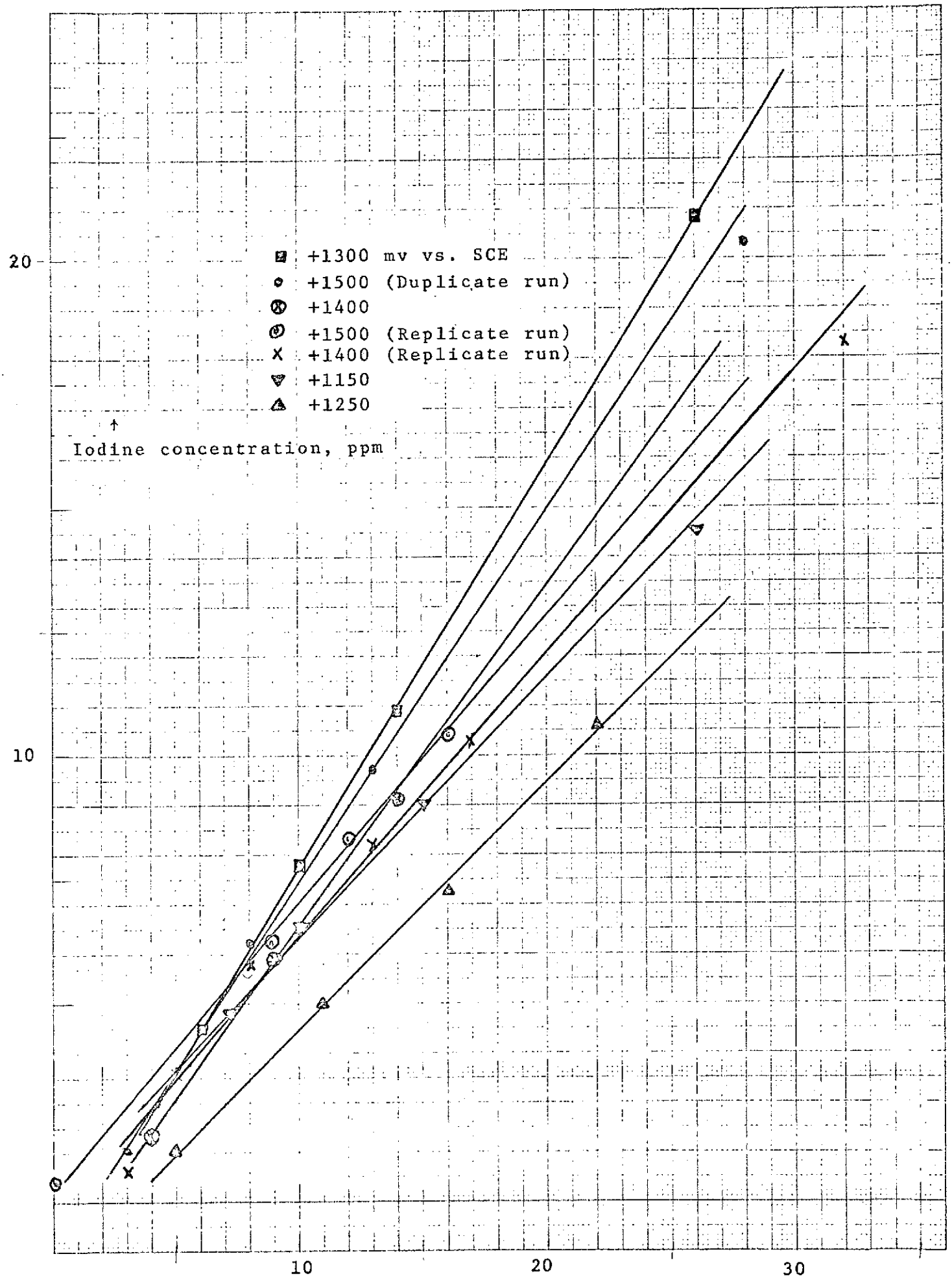
+1300 mv vs. SCE
+1500 (Duplicate run)
+1400
+1500 (Replicate run)
+1400 (Replicate run)
+1150
+1250
Iodine concentration, ppm
20
10
10
20
30
Time, minutes →

$I(H_2O)_x^+$, or to concurrent oxygen evoluation as well as oxidation of the oxide film on the stainless steel. The oxidation of the oxide film is discussed in more detail in another section of the report. Since the iodine meter measures only I_2 concentrations, another possibility is that the reaction $3I^- \rightarrow I_3^- + 2e$ is occurring simultaneously, and the I_3^- concentration is simply not being measured. Regardless of the reason, for any anamalous I_2 production it is desirable to keep the potential less anodic than +1100 mv vs. SCE. This provides maximum current efficiency and minimizes undesirable side reactions. It is imperative that the potential for these solutions be more anodic than 750 mv vs. SEC for the generation of iodine.

In addition to the iodine generation-time relationship, the current-time relationship was also measured. This data is shown in Figures 7 and 8. At a constant potential the current generally decreased with time until moderately stable limiting currents were obtained. These limiting currents were used to calculate the concentration in ppm anticipated after one minute. In Figure 9, these values for I_2 and I_3^- are compared to those found from the projected iodine rates. For each ppm of I_2 projected, 1.2 ppm is expected from the current measurements. For each ppm of I_3^- projected, 1.8 ppm is expected from the current measurements. The excess current may be consumed by any or a combination of the reasons listed previously. A

Figure 6.

Correlation between anodic polarization curve and measured iodine production rates. 500 ppm KI(382 I^-). Stirrer set at 10 volts. 321 Stainless Steel anode. The electrochemical cell was electrically grounded. Room conditions.

A. Iodine production rates calculated assuming the reaction: $2I^- \rightarrow I_2 + 2e$

x From the polarization curve

Ø From the Beckman iodine meter.

B. Iodine production rates calculated assuming the reaction: $3I^- \rightarrow I_3^- + 2e$

• From the polarization curve

Δ From the Beckman iodine meter

Fig. 6

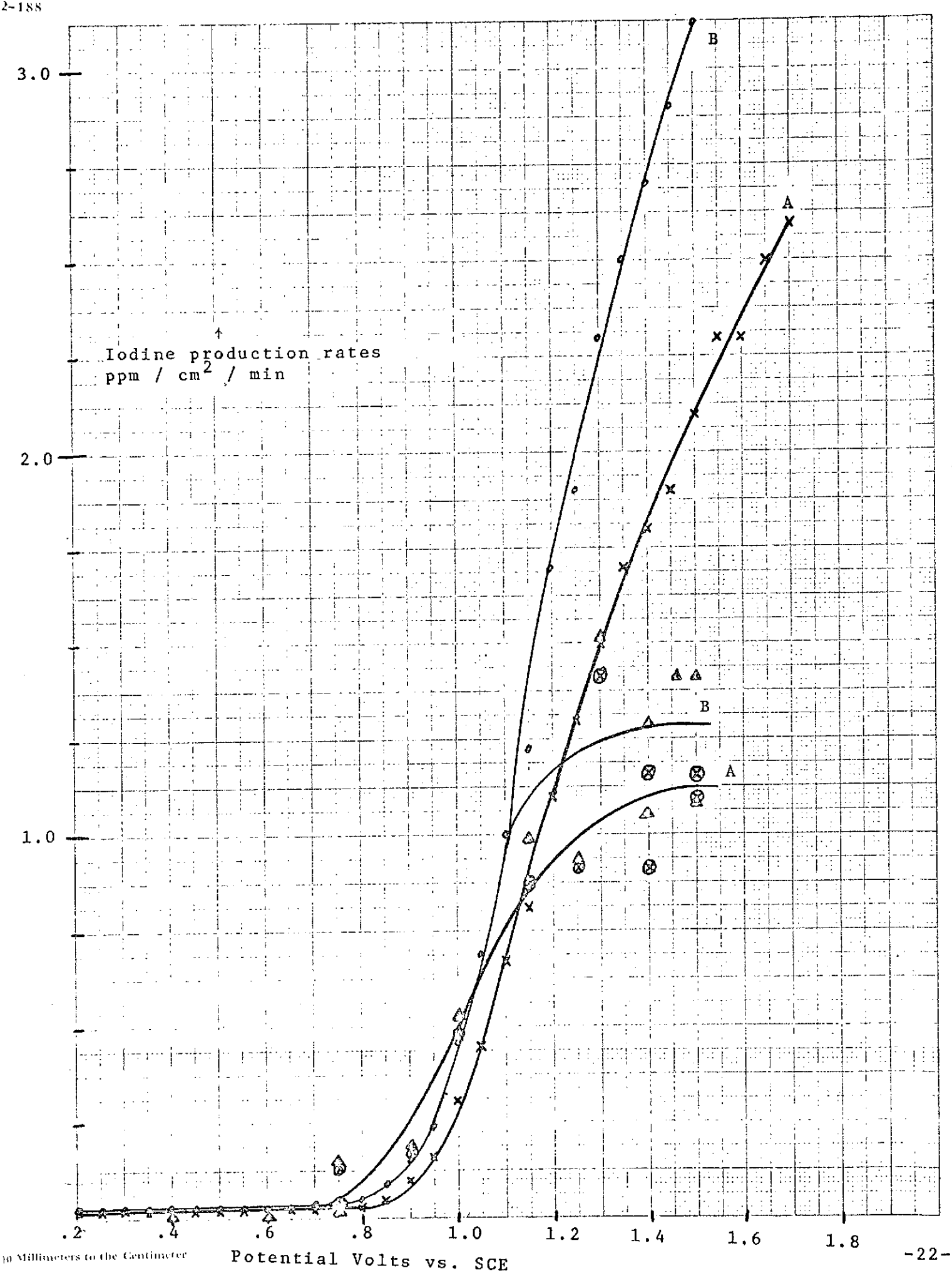

10 Millimeters to the Centimeter

TABLE II.

Iodine Production Rates
at Constant Anodic Potentials

Potential (mv vs. SCE)	Iodine Production Rate (ppm/min) A	B
+1300	0.76	0.82
+1500	0.66	0.76
+1400	0.66	0.69
+1500	0.58	0.58
+1400	0.49	0.57
+1150	0.47	0.53
+1250	0.49	0.50
+1000	0.26	0.28
+900	0.10	0.10
+750	0.08	0.08
+750	0.01	0.01
+600	0	0
+400	0	0

Where A assumes $2I^- \rightarrow I_2 + 2e$

and

B assumes $3I^- \rightarrow I_3^- + 2e$

Figure 7.

Change of current with time at constant anodic potentials. Room conditions. 500 ppm KI (382 ppm I^-)$_2$ Stirrer at 10v. Electrode area was 0.54 cm^2. Anode was 321 stainless steel.

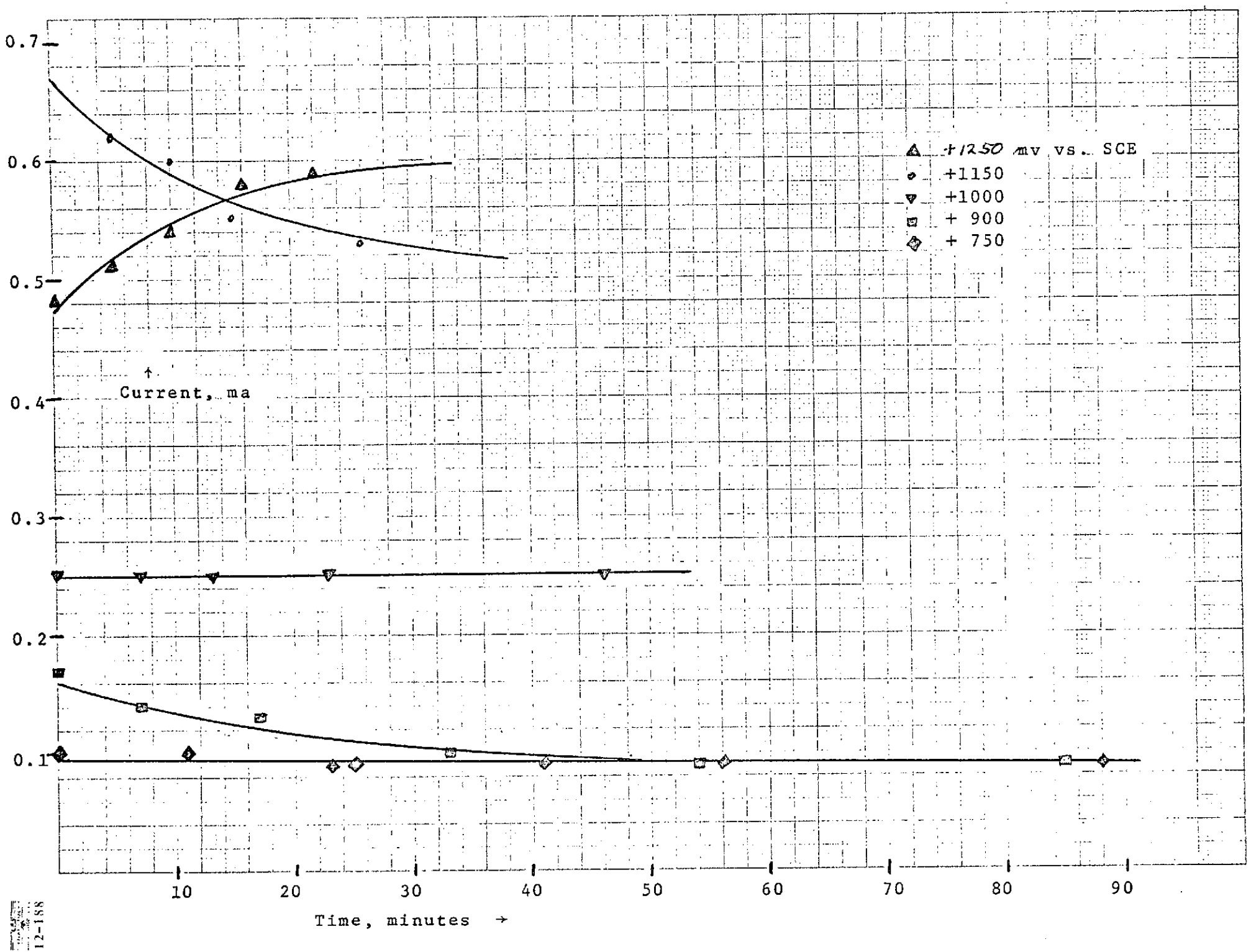

Figure 7.

12-188

10 millimeters to the Centimeter

Figure 8.

Change of current with time at constant anodic potentials. Same conditions as in Figure 5.

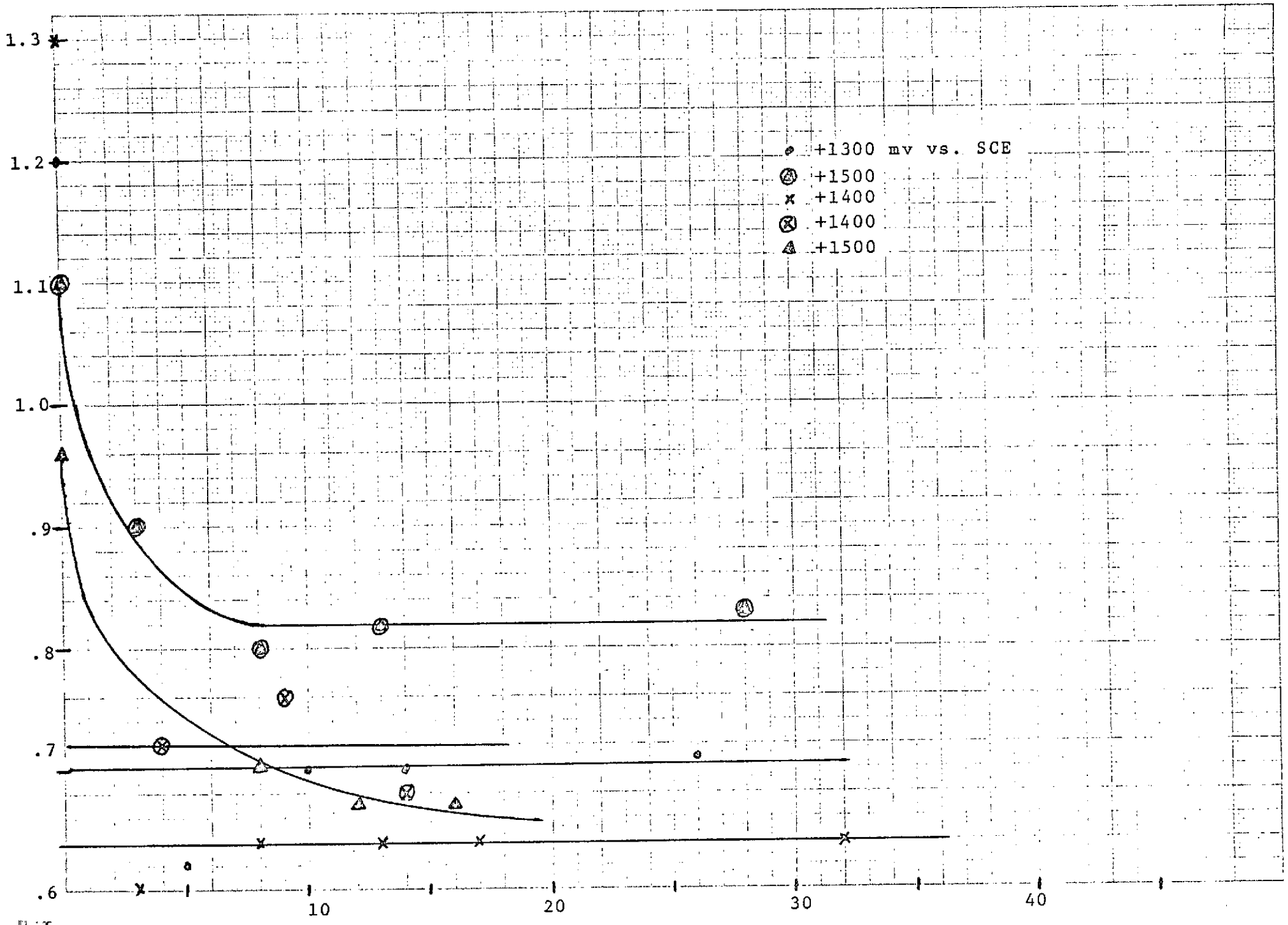

Figure 8.

more precise one-to-one relationship is obtained if I_2 is used as the reaction product. In the presence of I^-, there is a strong tendency for I_2 to form I_3^-. In the dilute solutions employed (maximum of 382 ppm I^-), the concentration of I^- may be so small that there is little probability of I_3^- production.

Effect of Iodide Concentration

A large iodine production rate for a 382 ppm I^- concentration was measured at +1300 mv vs. SCE. This potential was chosen as a convenient point at which to measure iodine production rates in a series of iodide concentrations ranging from 382 to 19 ppm. As shown in Figure 10A and 10B, I_2 and I_3^- rates decreased as the initial iodide concentration decreased. The I_2 and I_3^- production rates at each iodide concentration are ahown in Table III. From the current-time relationship shown in Figure 11, limiting currents were estimated and used to calculate the ppm of I_2 and I_3^- expected per minute. A linear relationship is shown in Figure 12 between I_2 and I_3^- concentrations obtained from both current and iodine meter measurements and iodide concentrations. A closer one-to-one relationship was found when I_2 is presumed to be the reaction product.

Influence of Electrode Geometry

All the work reported thus far was done on a 0.54 cm^2 piece of 321 Stainless Steel. A new, fluted electrode was constructed from a rectangular piece of 2 mil stainless steel, as

Figure 9.

Comparison of measured iodine production rates at constant potentials with those expected from current measurements.

- Calculated assuming the reaction

$$3I^- \rightarrow I_3^- + 2e$$

x Calculated assuming the reaction

$$2I^- \rightarrow I_2 + 2e$$

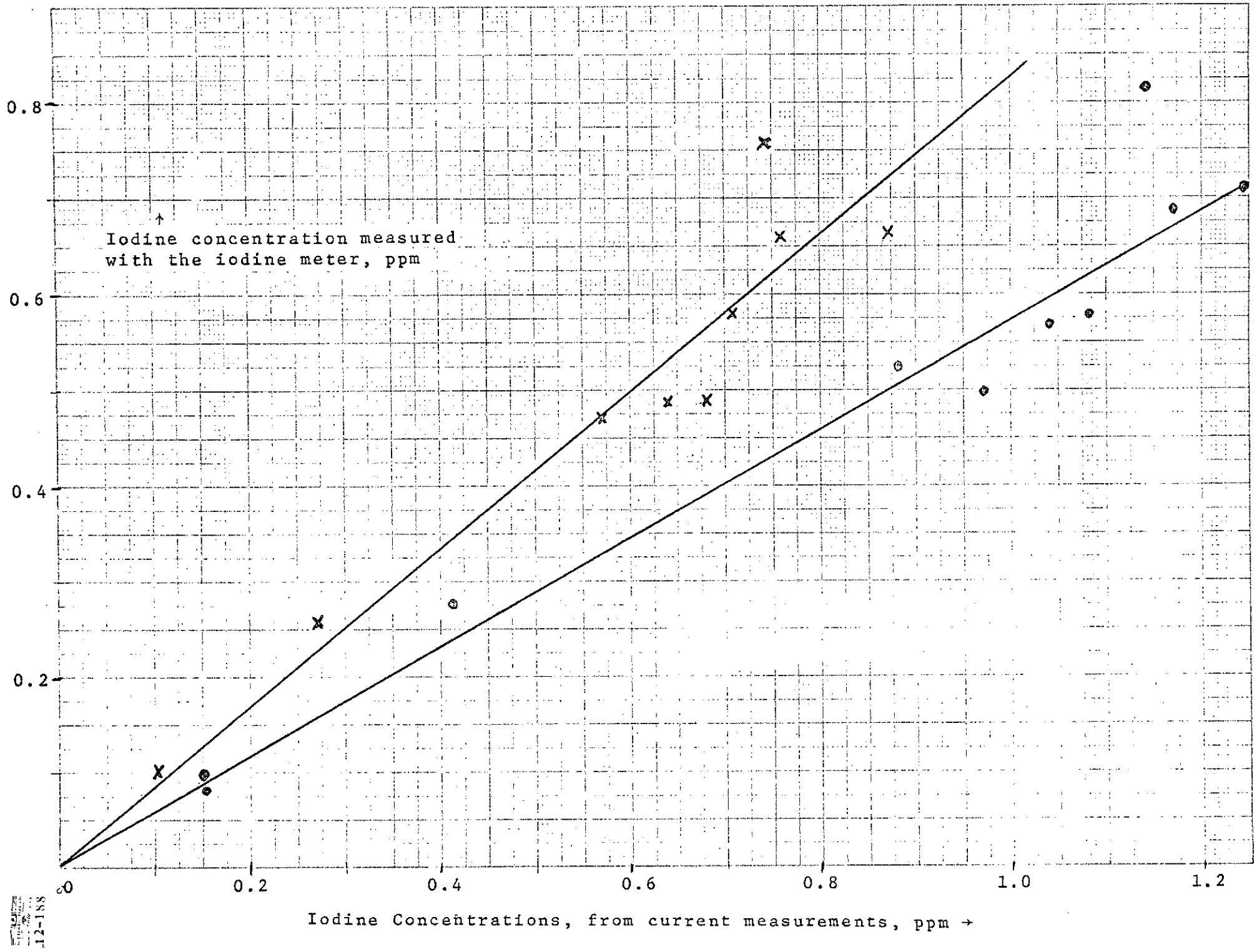

Figure 9.

Figure 10.

Effect of I^- concentration upon iodine production rates at constant potential (+1300 mv vs. SCE). Room conditions. Stirrer at 10v. Surface area = 0.54 cm^2. Anode was 321 stainless steel. Iodine concentrations are based on a constant initial iodide concentration.

A. Assuming the reaction $2I^- \rightarrow I_2 + 2e$

B. Assuming the reaction $3I^- \rightarrow I_3^- + 2e$

A.

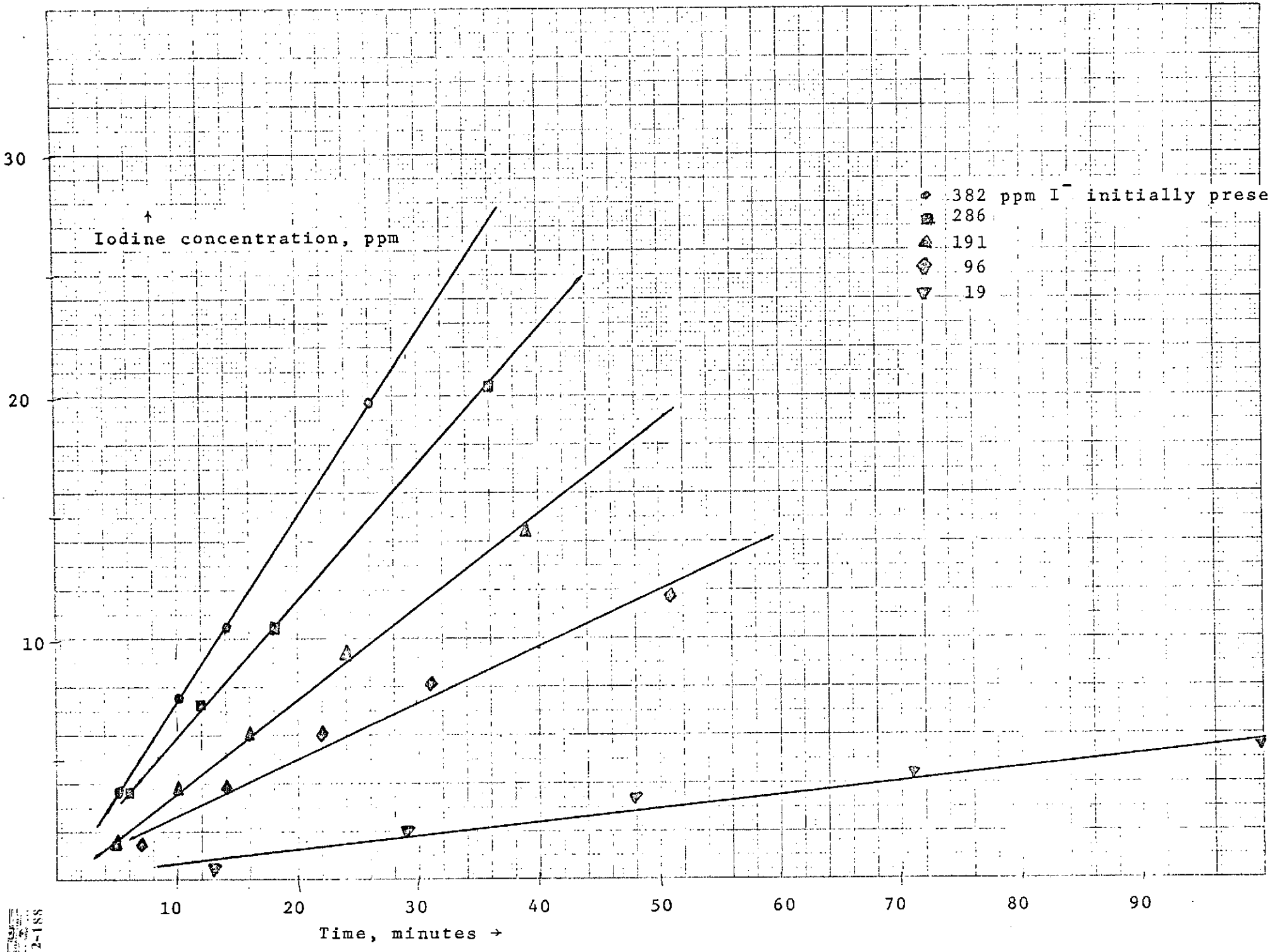

Figure 10

12-188

10 Millimeters to the Centimeter

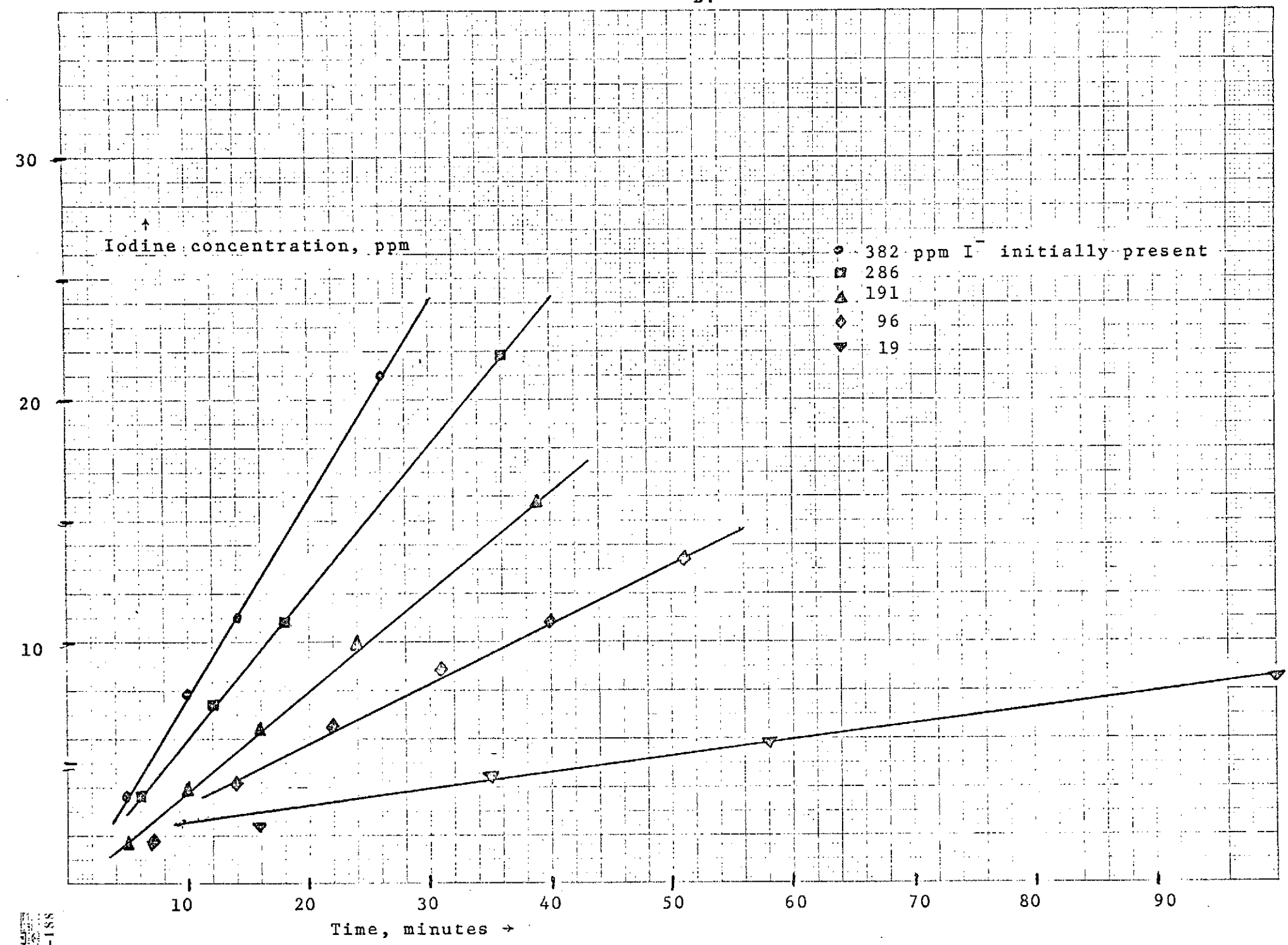

TABLE III.

Iodine production rates at different iodide concentrations at a constant potential of +1300 mv.

I^- conc. ppm of I^- initially present	Iodine production rates (ppm/minute)	
	A.	B.
382	0.76	0.81
286	0.57	0.59
191	0.39	0.41
96	0.24	0.24
19	0.06	0.06

Figure 11.

Change of current with time at different iodide concentrations at +1300 mv vs. SCE. Room conditions. Stirrer set a 10v. Surface area = 0.54 cm^2. Anode was 321 stainless steel.

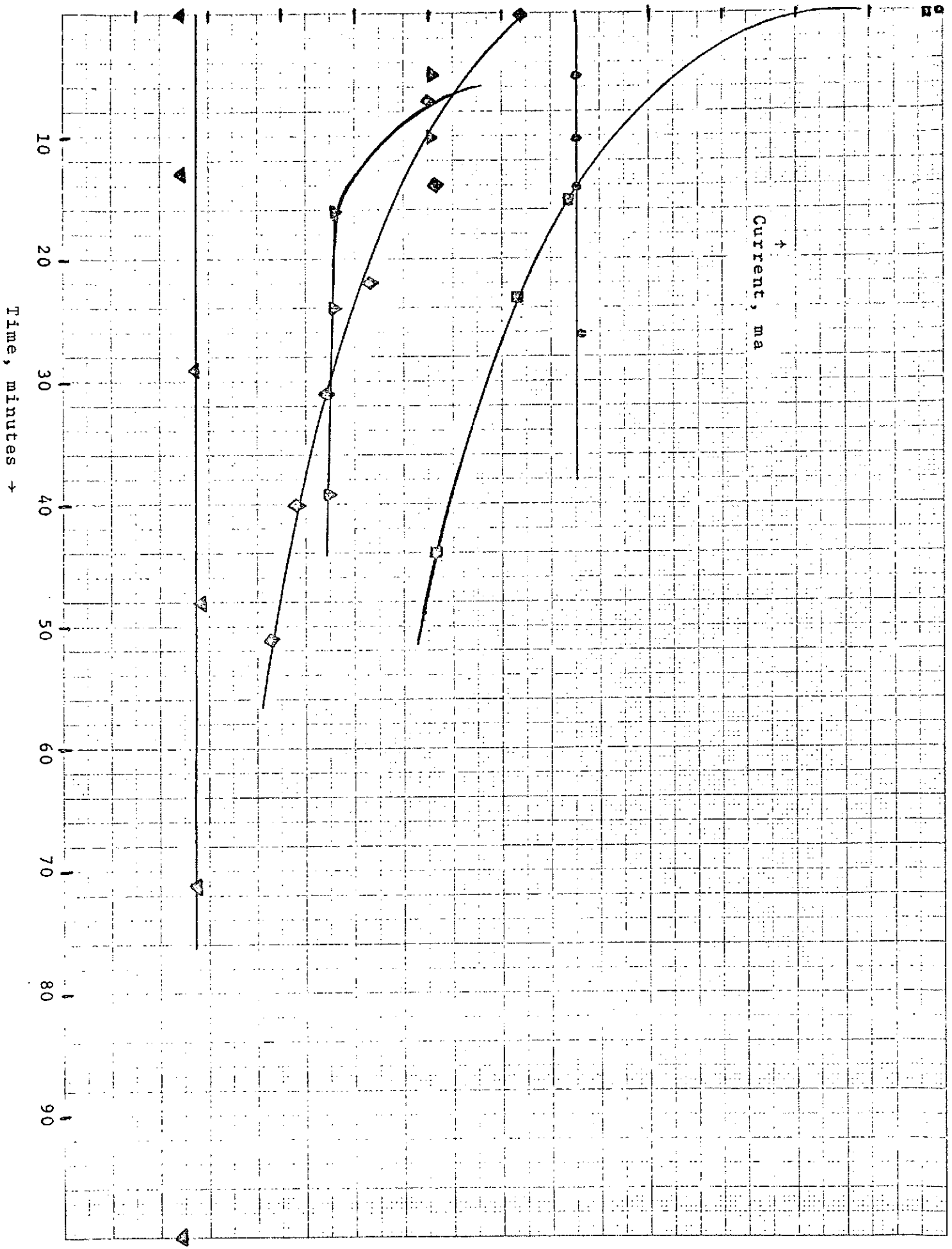

Figure 11.

Figure 12.

Change of iodine production rates with iodide concentrations at +1300 mv vs. SCE.

- ▣ Calculated from current measurements assuming the reaction $2I^- \rightarrow I_2 + 2e$
- ▲ Calculated from current measurements assuming the reaction $3I^- \rightarrow I_3^- + 2e$
- ⊗ Measured with the Beckman iodine meter assuming the reaction $2I^- \rightarrow I_2 + 2e$
- ● Measured with the Beckman iodine meter assuming the reaction $3I^- \rightarrow I_3^- + 2e$

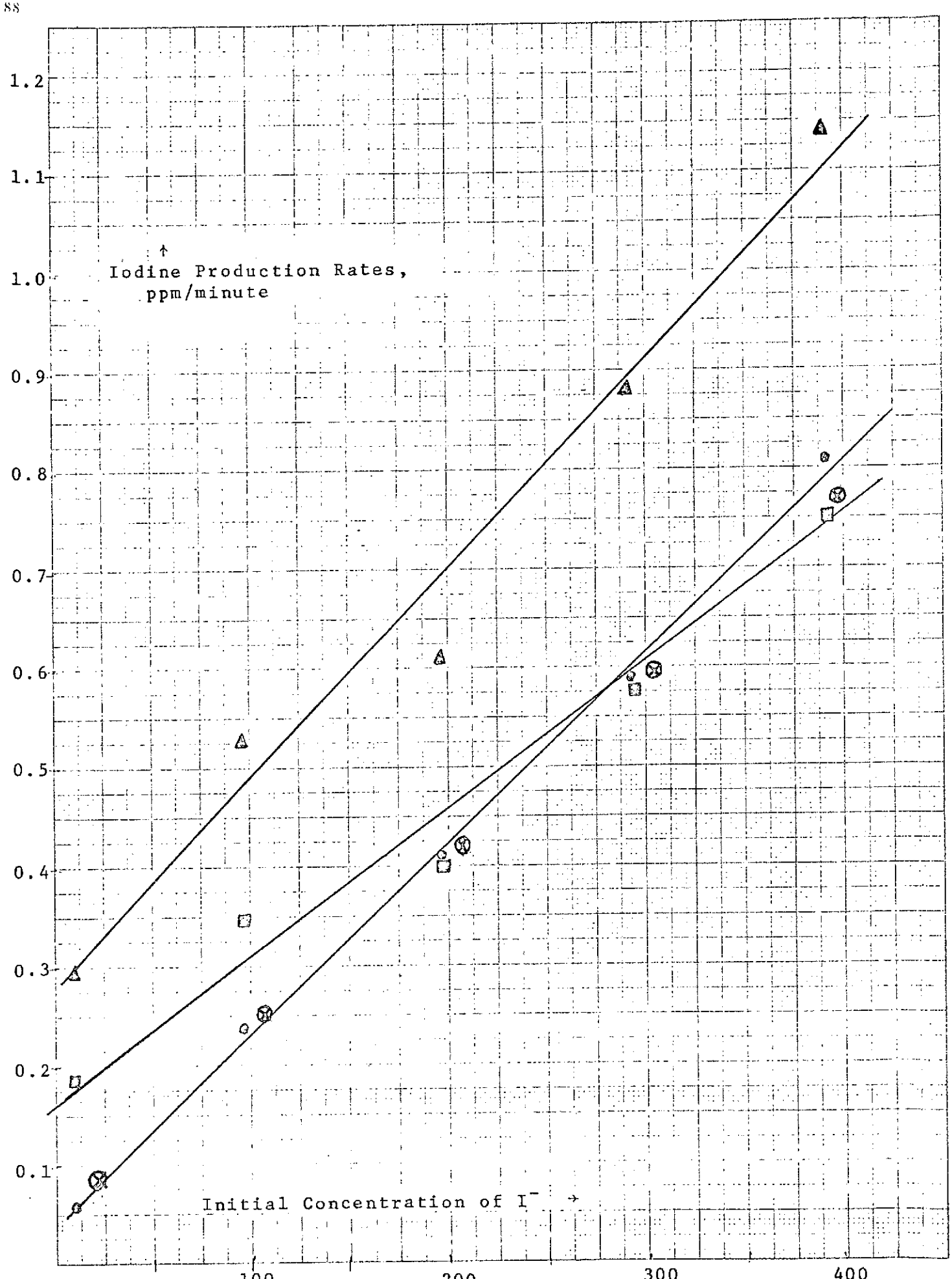

10 Millimeters to the Centimeter

Figure 12.

represented by Figure 13A. The area of this new electrode was 7.32 cm^2 compared to 0.54 cm^2 for the flat electrode represented in Figure 13B. Iodine production rates were observed to be influenced more by the geometric relationship between the smaller working electrode and the reference electrode. When the fluted electrode was positioned approximately 0.5 cm from the reference electrode as illustrated in Figure 14A, the iodine production rate from a solution containing 382 ppm I^- was 0.14 ppm/min cm^2 at 0.54 cm^2 electrode. When the fluted electrode was placed as close to the reference electrode as possible, as represented by Figure 14B, the measured current increased to 3.8 ma. This curren corresponded to an iodine production rate of 0.55 ppm/min/cm^2 shown in Figure 13C. The relative position of the electrode, therefore, alters the iodine production rate. However, when the position was maintained constant and the fluted electrode was compressed and/or stretched, no change in the iodine production rate was observed.

Polarization Curves of 321 Stainless Steel in Dilute KI Solutions

Much of the work was done on stainless steel working electrodes under anodic polarization; however, cathodic polarization curves were also run and typical data for unstirred solutions is shown in Figure 15. In solutions containing only KI and deaerated with an inert gas to remove oxygen, the only re-

Figure 13

Effect of electrode shape and size upon iodine production rates from 382 ppm I^- solutions.

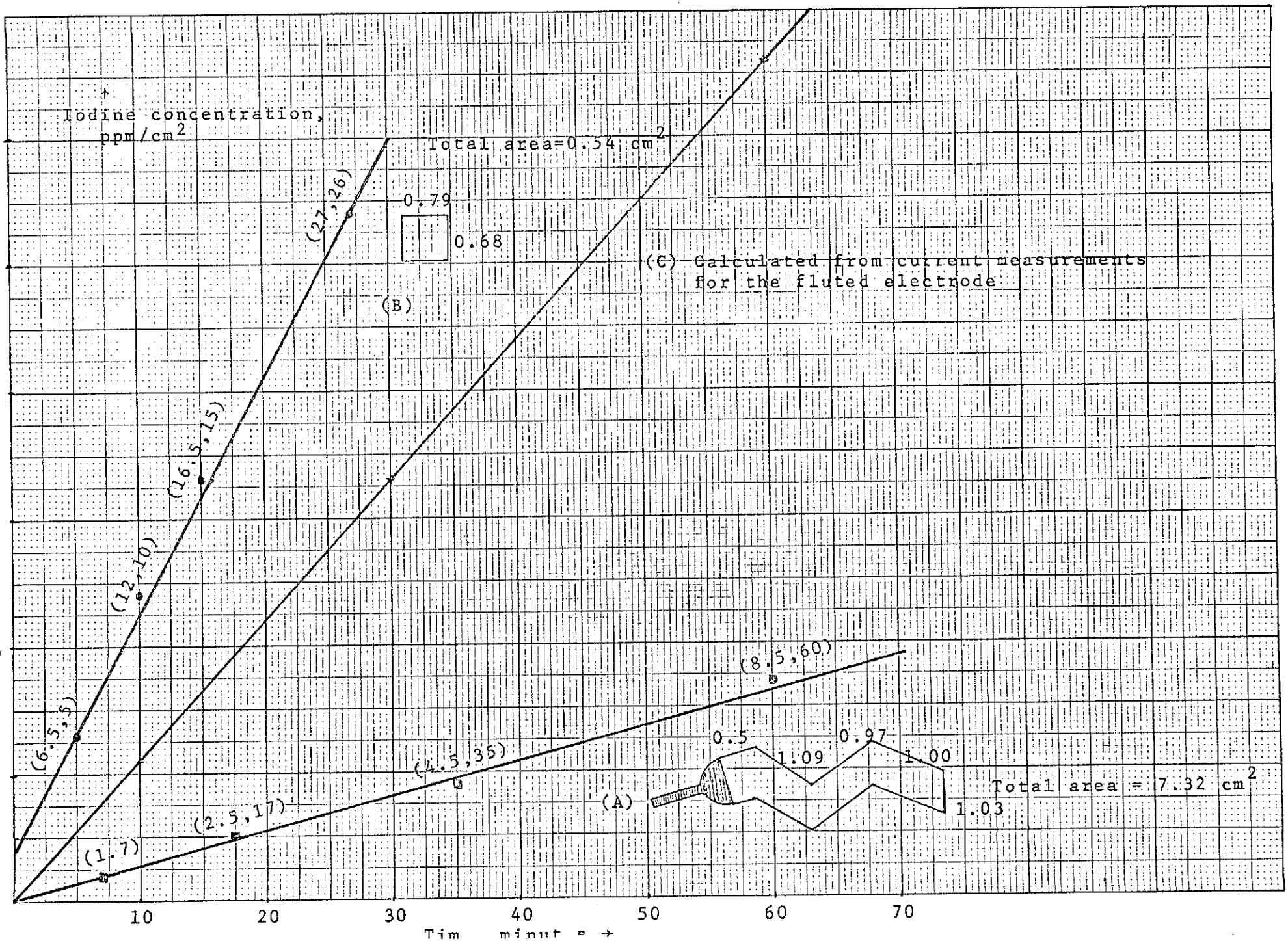
Iodine concentration, ppm/cm2
30
20
10
Total area=0.54 cm2
0.79
0.68
(27,26)
(16.5,15)
(12,10)
(6.5,5)
(1,7)
(2.5,17)
(4.5,35)
(8.5,60)
(B)
(C) Calculated from current measurements for the fluted electrode
(A)
0.5
1.09
0.97
1.00
1.03
Total area = 7.32 cm2
10
20
30
40
50
60
70
Tim minut s →

Figure 13

Figure 14.

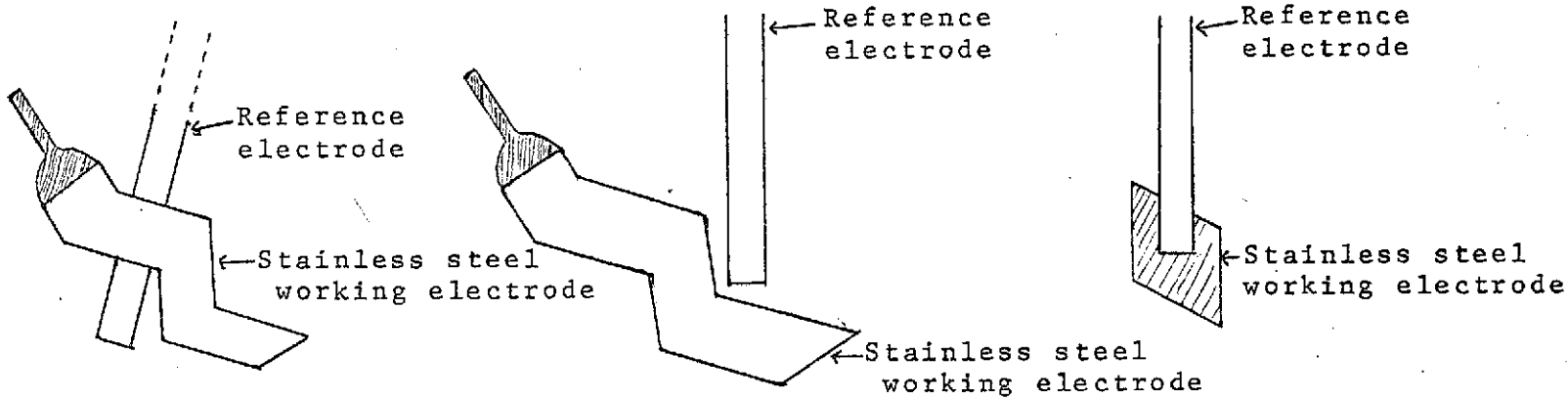

(A) Distance between the reference and working electrodes was 0.5 cm, (Area was 7.32 cm^2)

(B) Distance between the reference and working electrodes was 0.1 cm..

(C) Distance between the reference and working electrodes was 0.1 cm., (Area was 0.54 cm^2)

Figure 15.

Cathodic Polarization Curves

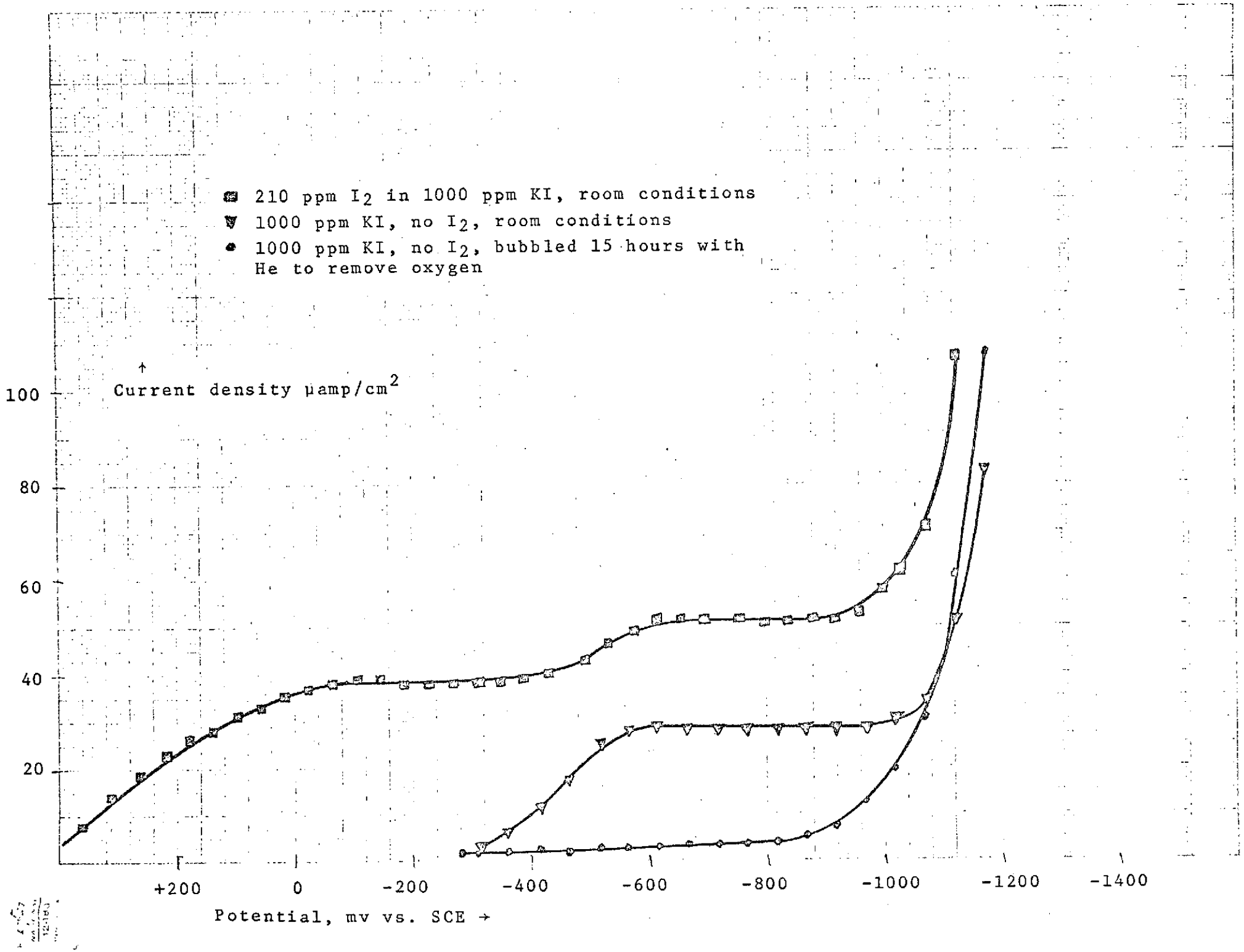
210 ppm I_2 in 1000 ppm KI, room conditions
1000 ppm KI, no I_2, room conditions
1000 ppm KI, no I_2, bubbled 15 hours with He to remove oxygen
Current density μamp/cm^2
100
80
60
40
20
+200
0
-200
-400
-600
-800
-1000
-1200
-1400
Potential, mv vs. SCE →

Fig. 15

duction reaction evident was hydrogen evolution near -1000 mv vs. SCE. The presence of oxygen in the solution caused a reduction wave near -400 mv. The presence of iodine caused another reduction wave which started at open circuit. In the presence of both iodine and oxygen, both reduction waves were present prior to hydrogen evolution.

A typical potentiostatic polarization curve in a stirred solution containing 500 ppm KI is shown in Figure 16. The cathodic curve is similar to that in the unstirred solution. There was no reduction of iodine but starting near -400 mv, there was reduction wave which involved oxygen. Near -1000 mv hydrogen evolution began. With stirring the reduction involving oxygen increased and a less well defined diffusion limiting current was obtained. Between -0.2v and +0.3v, only small background currents were measured. At 0.6v, anodic currents increased due to the start of iodine production. The large anodic wave resulted from one or a combination of waves due to iodine production, oxygen evolution, iodine oxidation, and/or oxidation of the passive film on the stainless steel. With additional anodic polarization, clear bubbles of oxygen could be seen on the steel surface.

Polarization Curves in Acidic Solutions

Anodic potentiostatic polarization curves were run for 321 stainless steel in acidic solutions as 1.0N H_2SO_4.

Figure 16.

Typical Potentiostatic Polarization Curve

Typical Potentiostatic Polarization Curve

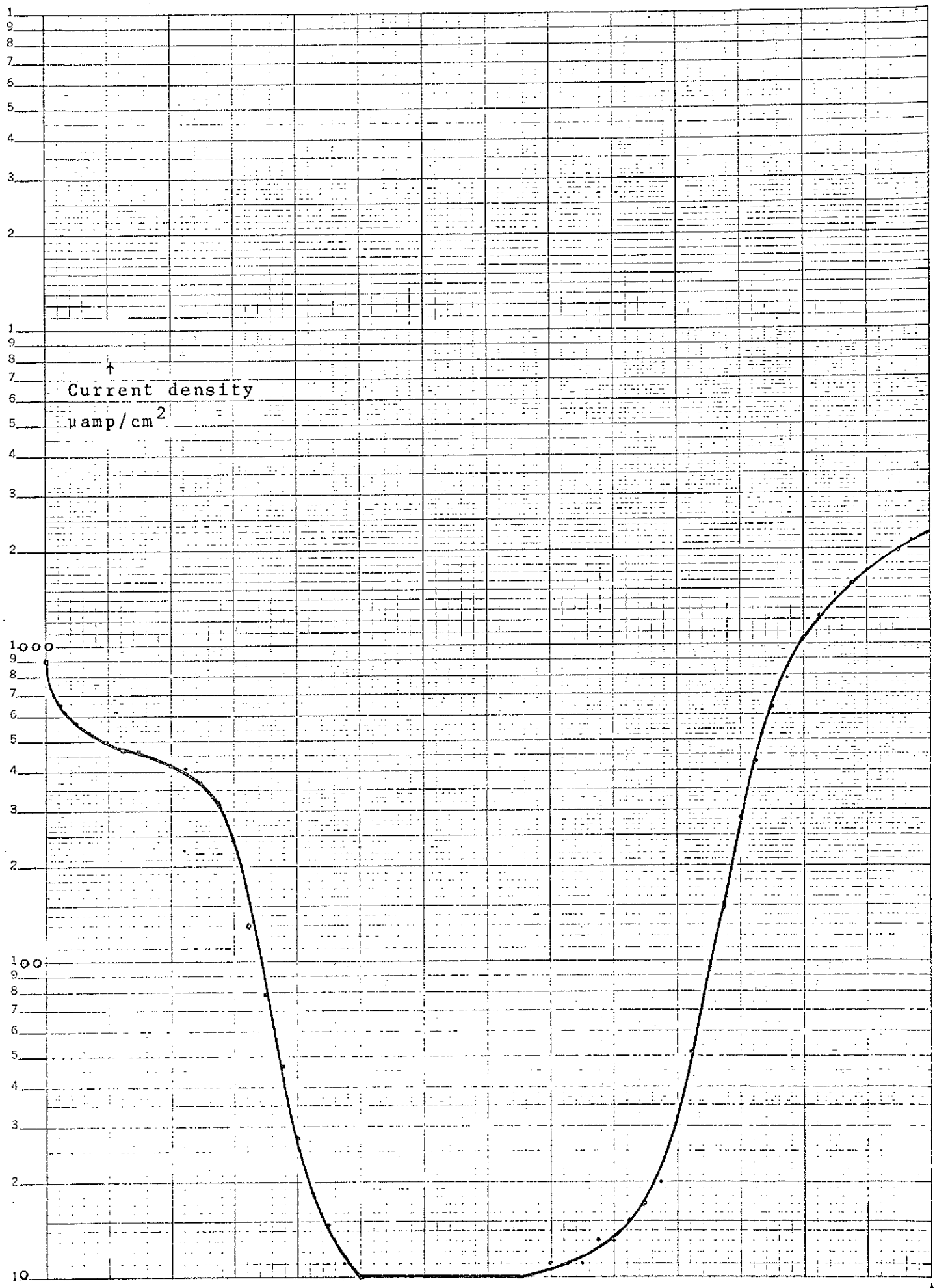

Semi-Logarithmic
4 Cycles x 10 to the inch

As shown in Figure 17, the presence of oxygen had little influence on the general shape and geometry of the anodic curves. In both cases no passive peaks were observed. Anodic currents first increased slowly due to slow dissolution and replacement of the surface film or to transport of ions through an imperfectly formed film. This slow current increase is not characteristic of an active corrosion process. At +850 mv vs. SCE, anodic currents increased rapidly with a Tafel slope of approximately 100 mv per current decade. A current peak was reached at +1350 mv. This peak is characteristic of high content stainless steels in acidic solutions and is believed to be due to oxidation of chromium from trivalent to the hexavalent form in the surface film. The hexavalent ion subsequenly dissolves. Such peaks have been shown by other researchers to increase with chromium content in the steel. The small current decrease indicates this new film is not very protective.

An increase in height of the current peak starting near +850 mv with increasing hydrogen ion concentration is shown in Figure 18. In a solution of 10 ppm KI in 0.1M $NaClO_4$ supporting electrolyte solution, no current peak was measured. In INH_2SO_4 currents in this peak region were almost three orders of magnitude larger than those observed in the 0.1M $NaClO_4$ solution. The peak currents in 3.6N H_2SO_4 were an order of magnitude

Figure 17.

Anodic potentiostatic polarization curves of 321 stainless steel in 1.0 N H_2SO_4

- ● Room conditions, oxygen present
- ▣ Oxygen removed by bubbling with argon

Figure 17

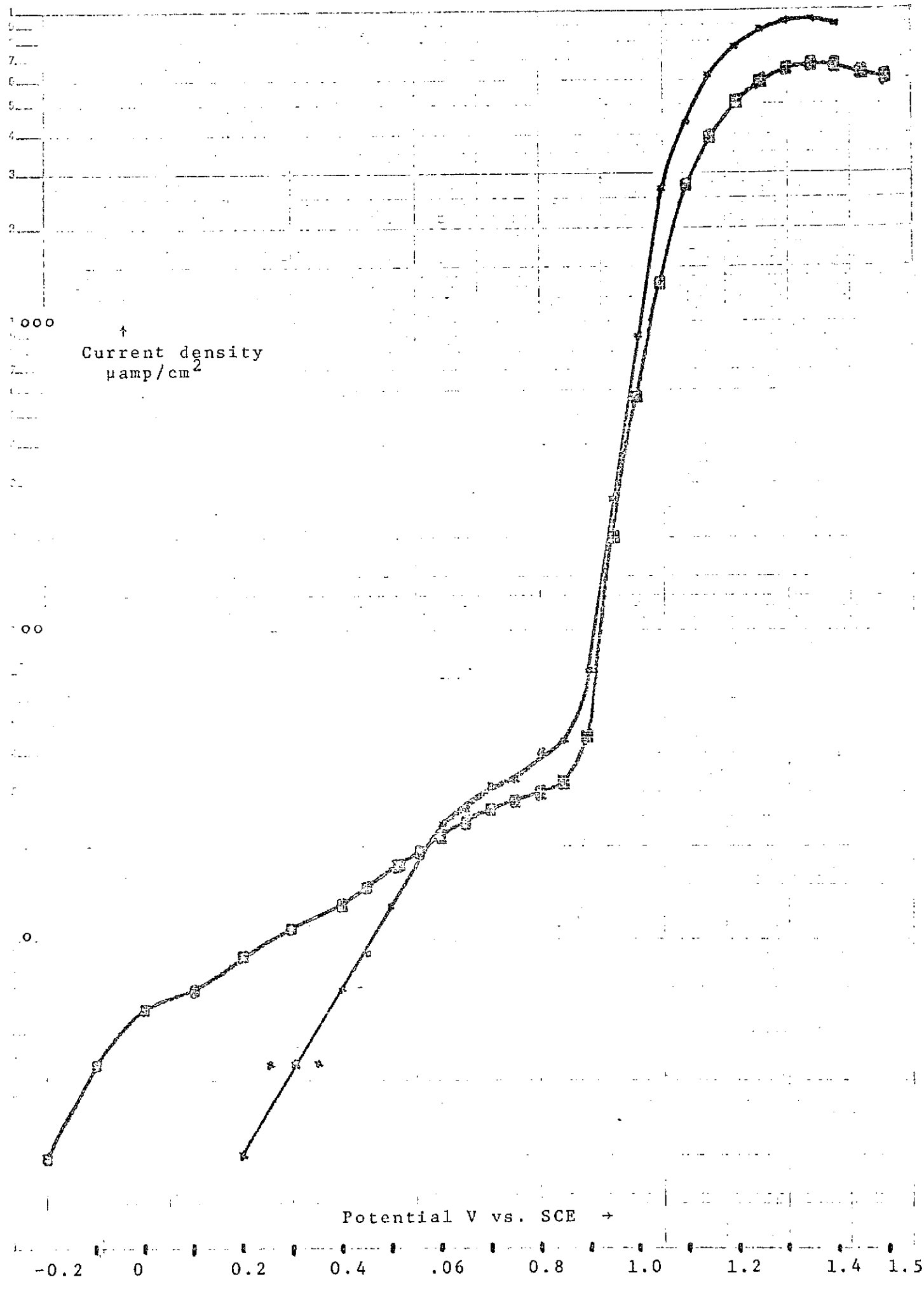
Current density
μamp/cm²
Potential V vs. SCE →
-0.2
0
0.2
0.4
.06
0.8
1.0
1.2
1.4
1.5

Figure 18.

Anodic potentiostatic polarization curves of 321 stainless steel bubbled with argon or helium to reduce oxygen concentrations.

= 3.6 N H_2SO_4

▲ 1.0 N H_2SO_4

● 10 ppm KI in 0.1M $NaClO_4$

Figure 18

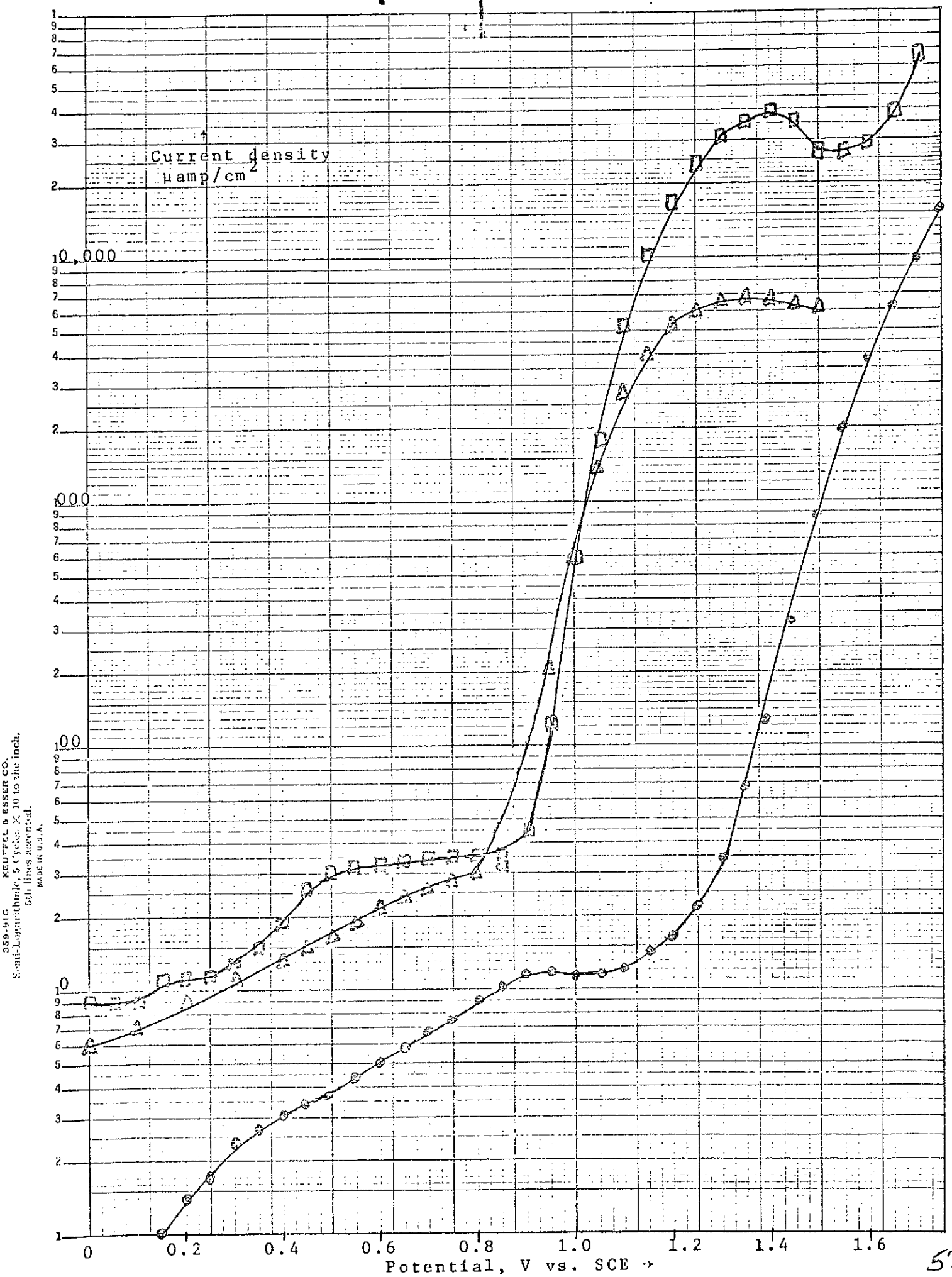

359-91G KEUFFEL & ESSER CO.
Semi-Logarithmic, 5 Cycles × 10 to the inch,
5th lines accented.
MADE IN U.S.A.

larger than in IN H_2SO_4.

Even though iodine was spontaneously liberated from 500 ppm KI in 3.6 N H_2SO_4, the anodic polarization curves in 3.6N H_2SO_4 and 3.6 N H_2SO_4 containing 500 ppm KI were measured and are shown in Figure 19. From open circuit to the chromium oxidation peak, anodic currents in the presence of KI were larger due to oxidation of iodide ions to iodine. Within experimental error, currents more anodic than +1100 mv were essentially the same regardless of the presence of KI and iodine.

In Figure 20, anodic potentiostatic polarization curves in 3.6 N H_2SO_4 and shown versus SCE and versus 321 stainless steel as reference electrodes. The general shapes of the curves are the same and parallel. For a given current the potential versus stainless steel was more positive than versus SCE. Similarities in the two curves indicate that stainless steel can be used as a suitable reference electrode.

In order to reduce the surface film before anodic polarization, the 321 stainless steel electrode was held at -440 mv vs. SCE for two minutes. At -400 mv vigorous hydrogen evolution was evident. When cathodic polarization was removed, the open circuit potential after five minutes stabilized

Figure 19

Anodic potentiostatic polarization curves of 321 stainless steel. Bubbled with argon to reduce oxygen concentration.

□ 3.6N H_2SO_4 + 500 ppm KI

• 3.6N H_2SO_4

Figure 19

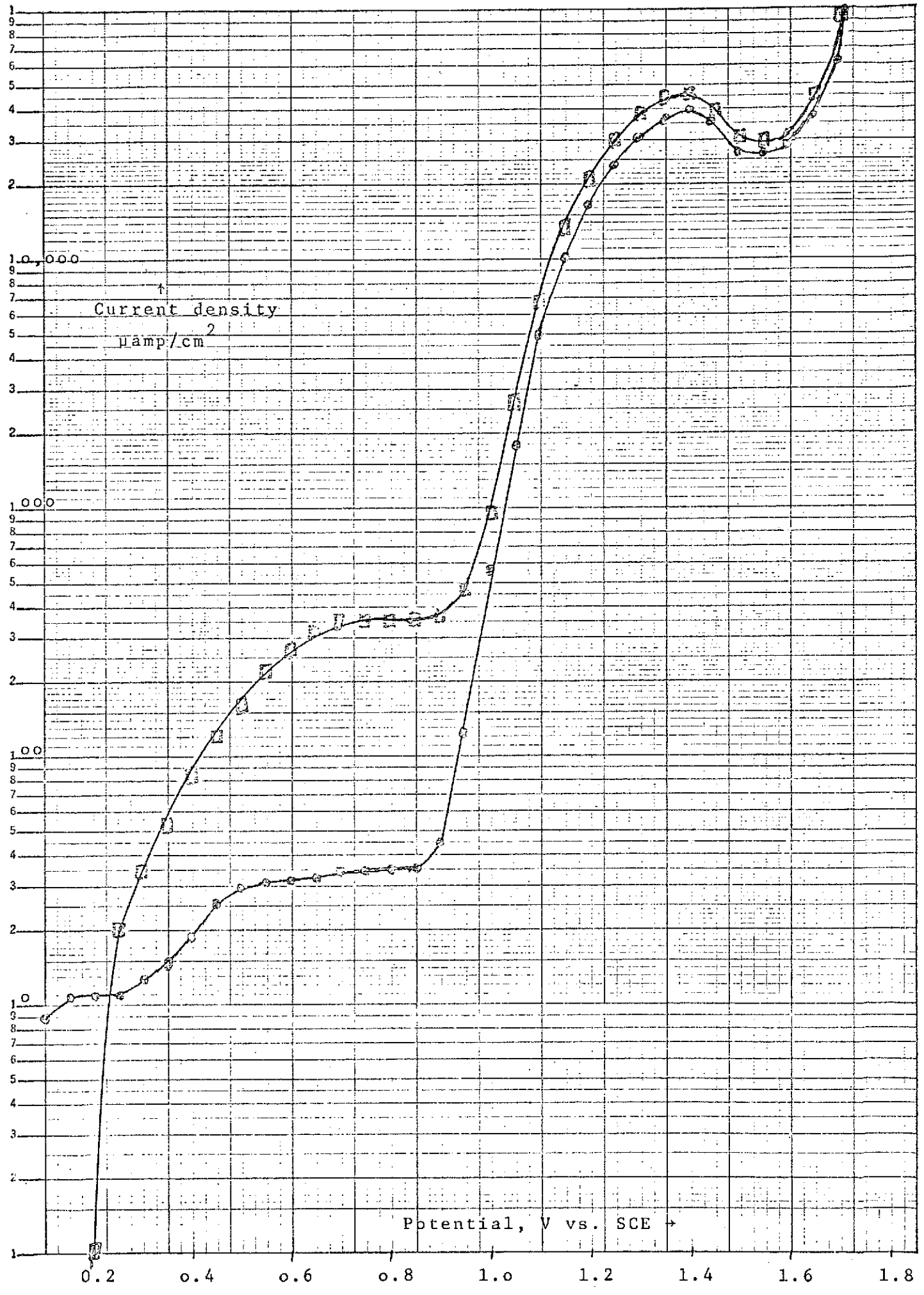

KEUFFEL & ESSER CO.
359-91G
Semi-Logarithmic, 5 Cycles X 10 to the inch,
6th lines accented.
MADE IN U.S.A.

Figure 20.

Comparison of anodic potentiostatic polarization curves of 321 stainless steel in 3.6N H_2SO_4. Bubbled with argon to reduce oxygen concentration.

□ vs. 321 Stainless steel

● Saturated calomel electrode

Figure 20

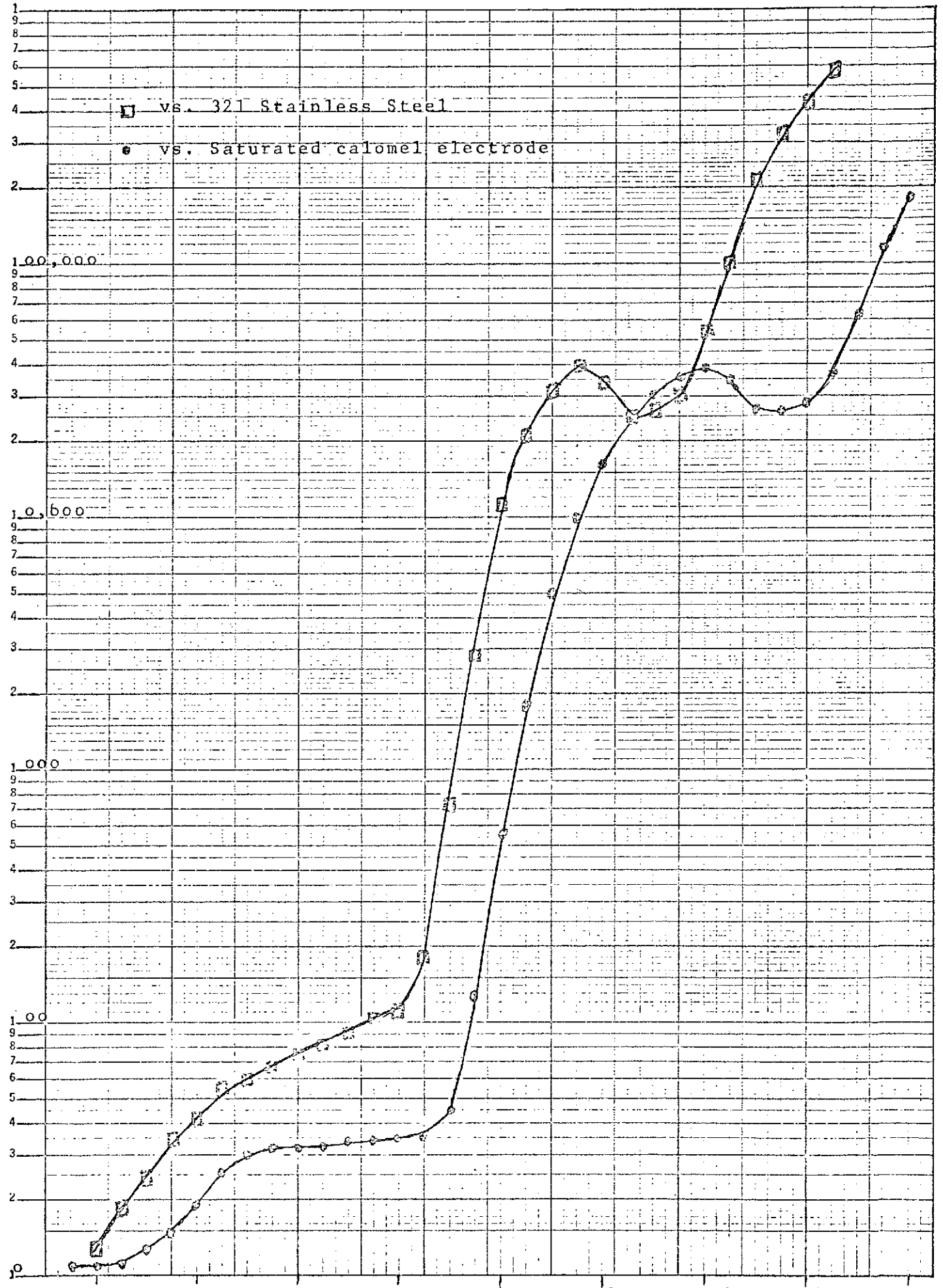

359-91G KEUFFEL & ESSER CO.
Semi-Logarithmic, 5 Cycles X 10 to the inch.
5th line is accented.
MADE IN U.S.A.

at -380 mv. At open circuit a black film began forming on the surface. When the potential was shifted to more anodic values at the rate of 5 mv per minute, a passive type of current-potential region was found, as shown in Figure 21. The current rapidly dropped from approximately 6,000/μamp/cm^2 to 80 μamp/cm^2. Over a 1.2v range the anodic current remained near 100 μamp/cm^2. This indicates slow dissolution but not true passivity of the surface. At 1.0v the current again increased rapidly due to chromium oxidation in the surface film. When the electrode potential was held at -400 mv for two minutes, a black film formed at first and then dissolved; then a reddish film formed and dissolved. The regions of potentials over which these events occurred are given in Figure 22.

Other workers have also found a strong dependence of anodic current density in the active-passive conversion region at the time of anodic treatment and pretreatment, particularly for alloys from 12.2% to 19.1% Cr. For these alloys the narrow active potential region extended from approximately -0.35 to -0.15v, and then only for electrodes electropolished and etched prior to immersion in the solution. It has been shown that there is a narrow active potential region in strong H_2SO_4 from -380 mv to -200 mv and only for electrodes cathodically reduced. As demonstrated in this work, as well as that of others, the electrodes electropolished and rinsed without etching were spontaneously passive upon immersion. This was indicated by

Figure 21.

Anodic potentiostatic polarization curves of 321 stainless steel in 3.6 N H_2SO_4.

Bubbled with argon. Held at -400 mv vs. SCE for two mintues before each run.

- ● Trial #1
- ▲ Trial #2

Figure 21

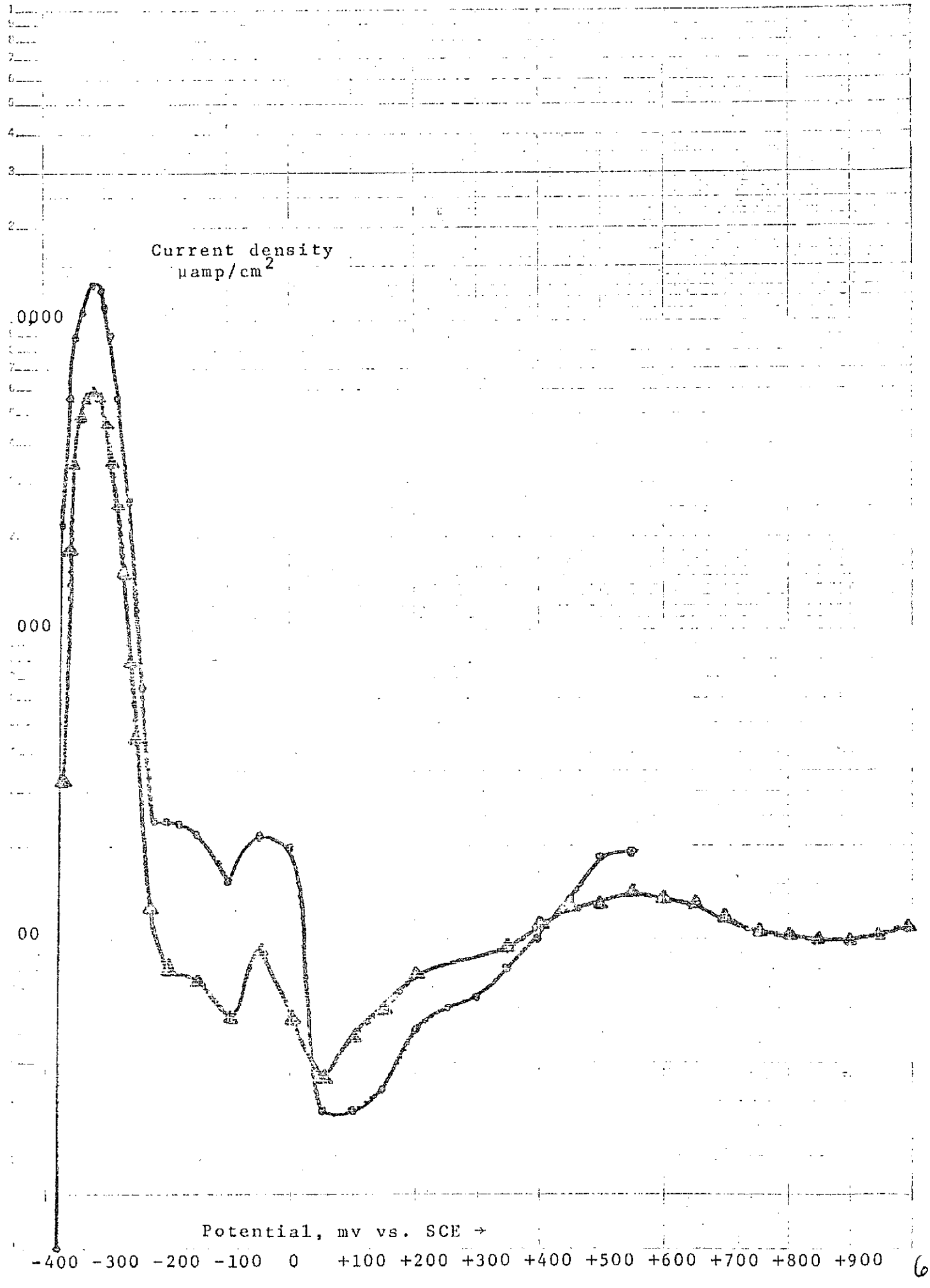
Current density
μamp/cm²
Potential, mv vs. SCE →
-400 -300 -200 -100 0 +100 +200 +300 +400 +500 +600 +700 +800 +900

Figure 22

Anodic potentiostatic polarization curves of 321 stainless steel in 3.6N H_2SO_4. Bubbled with argon.

□ No pre-treatment (cathodic)

● Cathodically held at -400 mv for two minutes

Figure 22.

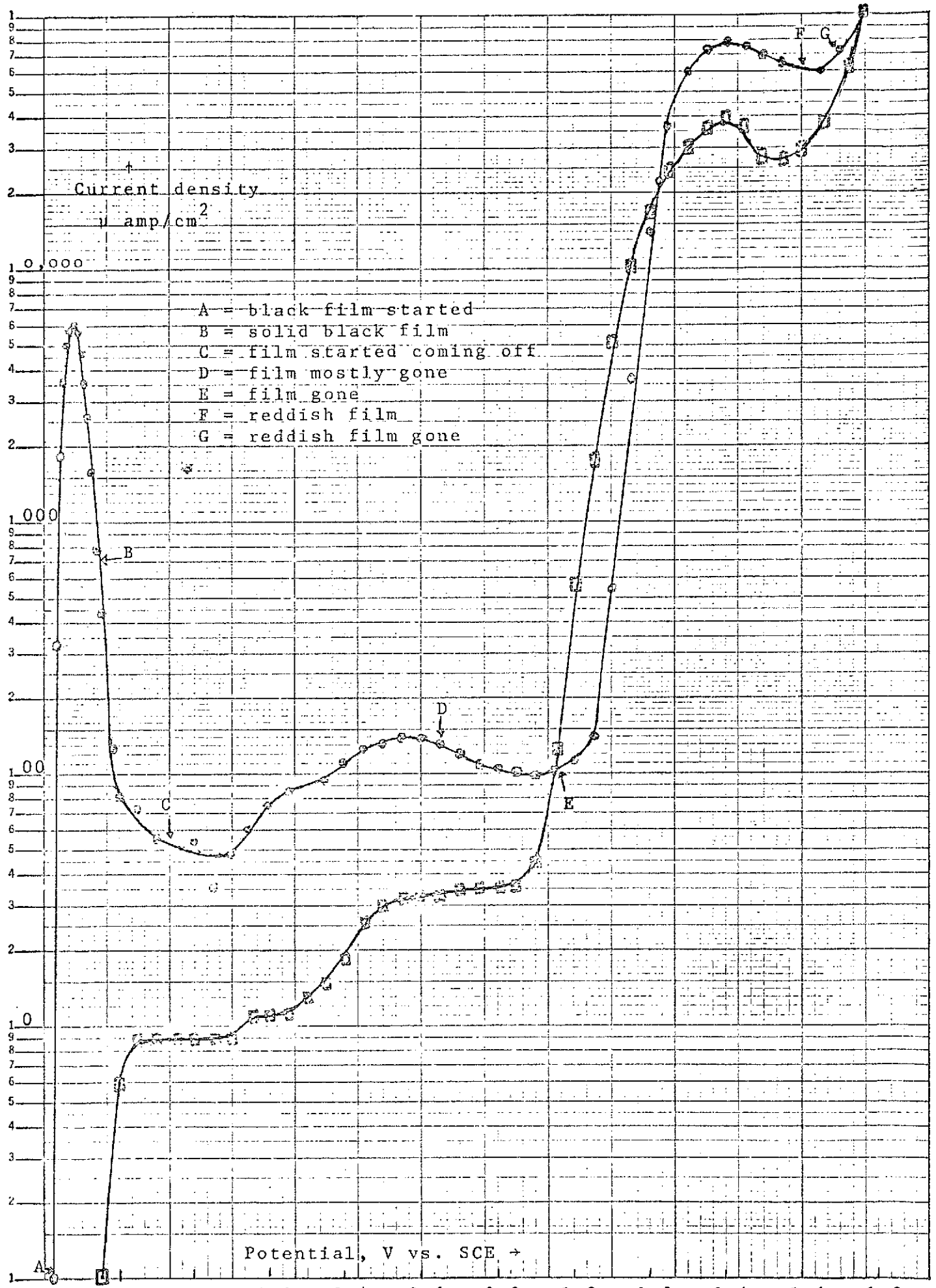

359-91C KEUFFEL & ESSER CO.
Semi-Logarithmic, 5 Cycles × 10 to the inch.
5th lines accented.
MADE IN U.S.A.

the absence of large amounts of anodic current flow upon shifting the electrode potential to more noble values and by an immersion potential more noble than -0.15v.

Polarization Curves of Stainless Steel

For actual Skylab sue, a more convenient and practical reference electrode than a saturated calomel electrode is desirable. Current-time and potential-time curves for Type 304 and 321, as well as a section of stainless steel bellows comparable to that to be used in the Skylab program were measured versus 304 and 431 stainless steel coupons as reference electrodes.

All the electrodes used are illustrated in Figure 23. Curve A of Figure 24 shows a continuous decrease of current with time for a 321 stainless steel working electrode (0.54 cm^2) versus a 304 reference electrode (8 cm^2) in a solution originally containing 500 ppm KI. Figure 24A gives an essentially constant potential-time relationship for these electrodes at an applied voltage of _1235 mv. At +1200 mv, some oxygen could be evolved, but most of the current has been demonstrated to be due to iodine production. As the iodide ion concentration decreases, the measured current decreases.

Curve B of Figure 24 is the current-time relationship for the metal bellows sample (7.81 cm^2) versus a 321 stainless

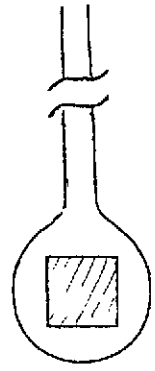

321 Stainless steel working electrode (0.54 cm^2)

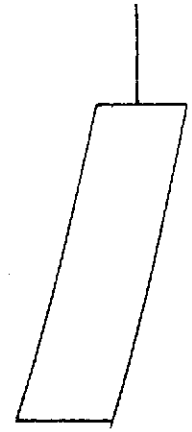

304 Stainless steel reference electrode (8 cm^2)

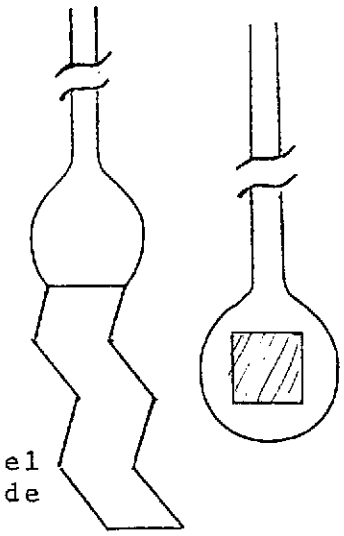

304 Stainless steel working electrode (7.03 cm^2)

321 Stainless steel reference electrode (0.54 cm^2)

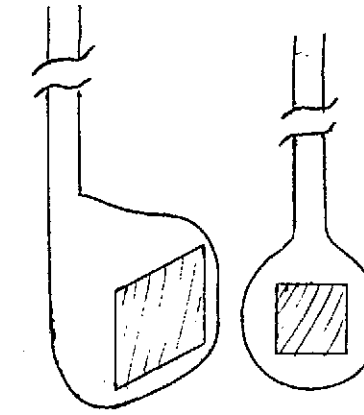

321 Stainless steel working electrode (2.89 cm^2)

321 Stainless steel reference electrode (0.54 cm^2)

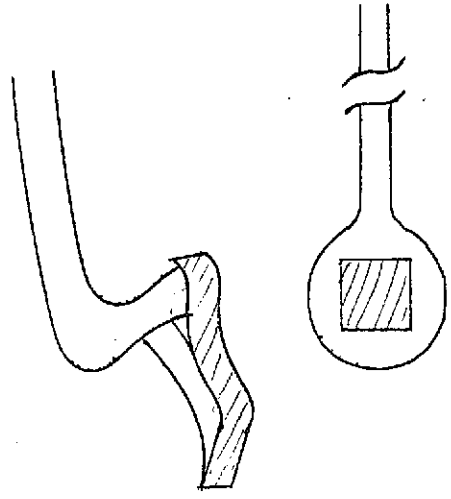

Spacecraft stainless steel working electrode (7.81 cm^2)

321 Stainless Steel electrode (0.54 cm^2)

Figure 23

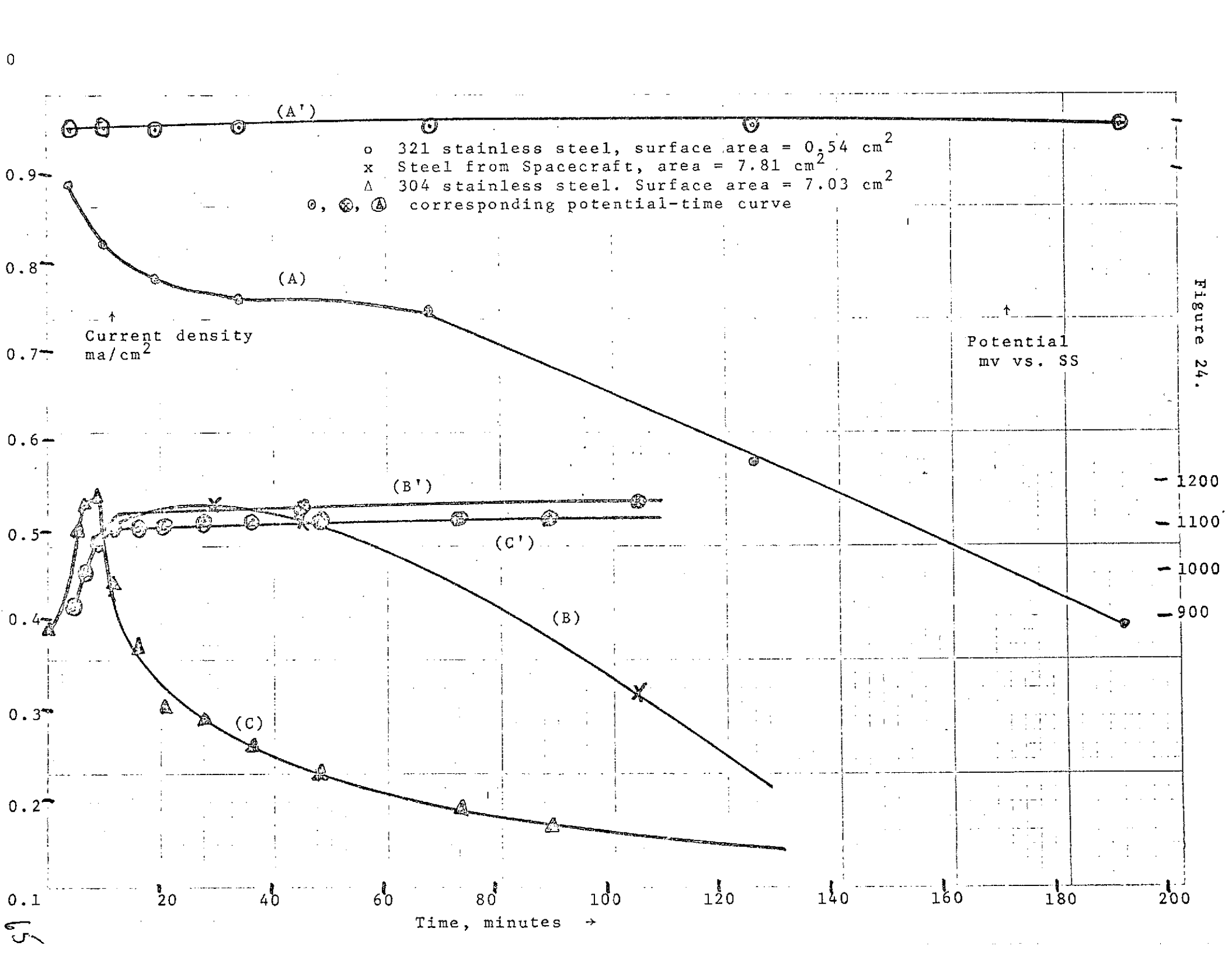
(A')
o 321 stainless steel, surface area = 0.54 cm²
x Steel from Spacecraft, area = 7.81 cm²
Δ 304 stainless steel. Surface area = 7.03 cm²
⊙, ⊗, Ⓐ corresponding potential-time curve
(A)
Current density
ma/cm²
Potential
mv vs. SS
(B')
(C')
(B)
(C)
0.9
0.8
0.7
0.6
0.5
0.4
0.3
0.2
0.1
1200
1100
1000
900
20
40
60
80
100
120
140
160
180
200
Time, minutes →

Figure 24.

steel reference electrode (.054 cm^2). For the first twenty minutes the current increases, but then decreases again with time as expected. Figure 24B shows the potential drift from 1040 mv to 1160 mv. After forty minutes the potential stabilized at approximately +1150 mv. The applied voltage was +1200 mv. The initial current increase paralleled this shift of potential to more anodic values. When the potential stabilized, the current decreased again as iodide ions were oxidized, the current decreased again as iodide ions were oxidized to iodine.

The initial increase of current and potential is shown even more clearly in Figure 2C and 2C'. After ten minutes the current decreased sharply with time. At sixteen minutes the potential stabilized at +1120 mv.

The current-time behavior for a larger piece of 321 stainless steel (2.89 cm^2) is shown in Figure 25A. For the first twenty-four minutes, the currents increase but then decreased sharply with time, as in the other experiments. However, in Figure 3A' the potential is seen to remain essentially constant at +1160 mv.

Curve B of Figure 25 exhibits a continued increase of current with time or a 304 stainless steel electrode (7.03 cm^2) versus a 321 stainless steel reference (0.54 cm^2). Curve B'

Figure 25

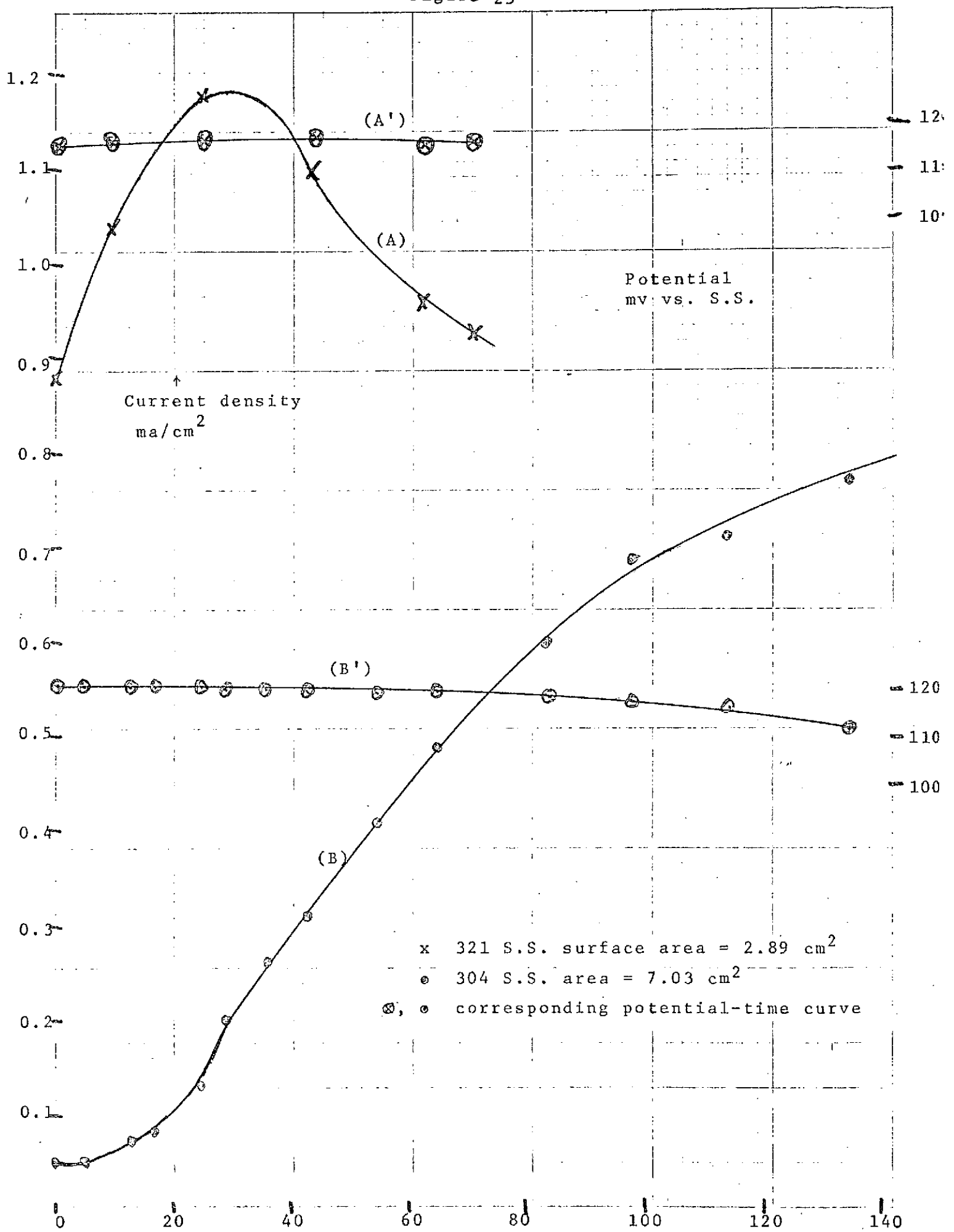
1.2
1.1
1.0
0.9
0.8
0.7
0.6
0.5
0.4
0.3
0.2
0.1
(A')
(A)
(B')
(B)
Potential
mv vs. S.S.
Current density
ma/cm2
x 321 S.S. surface area = 2.89 cm2
304 S.S. area = 7.03 cm2
corresponding potential-time curve
0
20
40
60
80
100
120
140
Time, minutes →

shows a shift of potential from +1210 mv to +1110 mv with time. For this experiment the applied voltage was set at +1130 mv. Both the current-time and potential-time relationships were opposite to those in reported previous experiments. The solution color was more brown than previous iodine solutions. When starch indicator was added to a sample, no deep blue color, characteristic of the iodine-starch complex was developed. The absence of iodine was verified with the iodine meter. A visual survey of the 304 stainless steel surface revealed pits in the steel surface and especially along the edges of the thin sheet electrode. The concentrations of iron and chromium were not measured in this experiment; however, dissolution of iron was evident.

The concentrations of iron and chromium from 321 and the bellows stainless steel when immersed in distilled water containing 500 ppm KI were measured as a function of time by atomic absorption spectrometry. When a 7.81 cm^2 sample of spacecraft stainless steel was polarized at a potential of -1160 mv for 106 minutes, the concentration of iron was found to be less than 0.05 ppm, and the chromium concentration was 0.113 ppm. When a sample of 321 stainless steel having an area of 3.89 cm^2 was polarized under the same conditions for two hours, the iron concentration was found to be 0.75 ppm, and the chromium concentration was 0.10 ppm.

Approximately 14 cm^2 sample of the metal bellows stainless steel was immersed in distilled water containing 10 ppm iodine. After 24 hours the iron concentration was 0.05 ppm, and chromium was observed to be 0.05 ppm. After 47 hours the iron concentration was calculated to be 0.10 ppm, and chromium concentration remained at 0.05 ppm. More data over longer periods of time is needed to firmly establish the corrosion rates. These preliminary values correspond to $3.6 \times 10^{-3} \frac{ppm}{cm^2}$ hr for the bellows stainless steel at +1160 mv, $130 \times 10^{-3} \frac{ppm}{cm^2}$ hr for the 321 stainless steel at +1160, and $0.2 \times 10^{-3} \frac{ppm}{cm^2}$ hr for the metal bellows in distilled water containing 10 ppm iodine at open circuit potential. Assuming uniform corrosion rates, these values correspond to iron dissolutions of 3.0×10^{-4} cm/yr for the metal at +1160 mv, 72×10^{-4} cm/yr for the 321 stainless steel at +1160 mv, and 0.17×10^{-4} cm/yr for the stainless steel at open circuit. Anodic polarization sharply increases the iron dissolution rate. This increase may have been due to the increased anodic oxidation of the passive film on the stainless steel discussed in the section on anodic polarization in corrosive solutions. Indeed, correlation curves have shown that at potentials more anodic than +1100 mv vs. SCE not all the current is consumed by iodine production. The additional current could be caused by some anodic dissolution of the stainless steel.

In all experiments the current densities for the 321 stainless steel were larger than those for 304 and the bellows stainless steel for the same length of time. For the 321 stainless steel, the sides and back were covered by an epoxy resin. For the thin 304 and bellows stainless steel strips, the backs and sides were exposed and total area measured. The differences in current densities were undoubtedly due to the higher efficiency for iodine production of the side facing the reference electrode.

Simulated Skylab Polarization Cell

In order to simulate actual Skylab tanks, the cell illustrated in Figure 26 was constructed. At +900 mv vs. a stainless steel reference electrode, no iodine was generated from distilled water containing 50 ppm KI (38 ppm I^-). At a potential of +1000 mv the concentration of iodine increased with time as shown in Figure 27 for both stressed and unstressed conditions. Stress was applied by screening down the plunger and thereby compressing the bellows. The unstressed condition showed a larger iodine production rate, 0.13 ppm/minute, compared to the stressed, 0.10 ppm/minute. In compressing the bellows the distance and therefore the resistance between the bellows and reference electrode was increased. Compression also decreased the area of the working electrode. Either of these factors could account for the decrease in iodine production.

Figure 26.

Simulated Skylab Water Tank

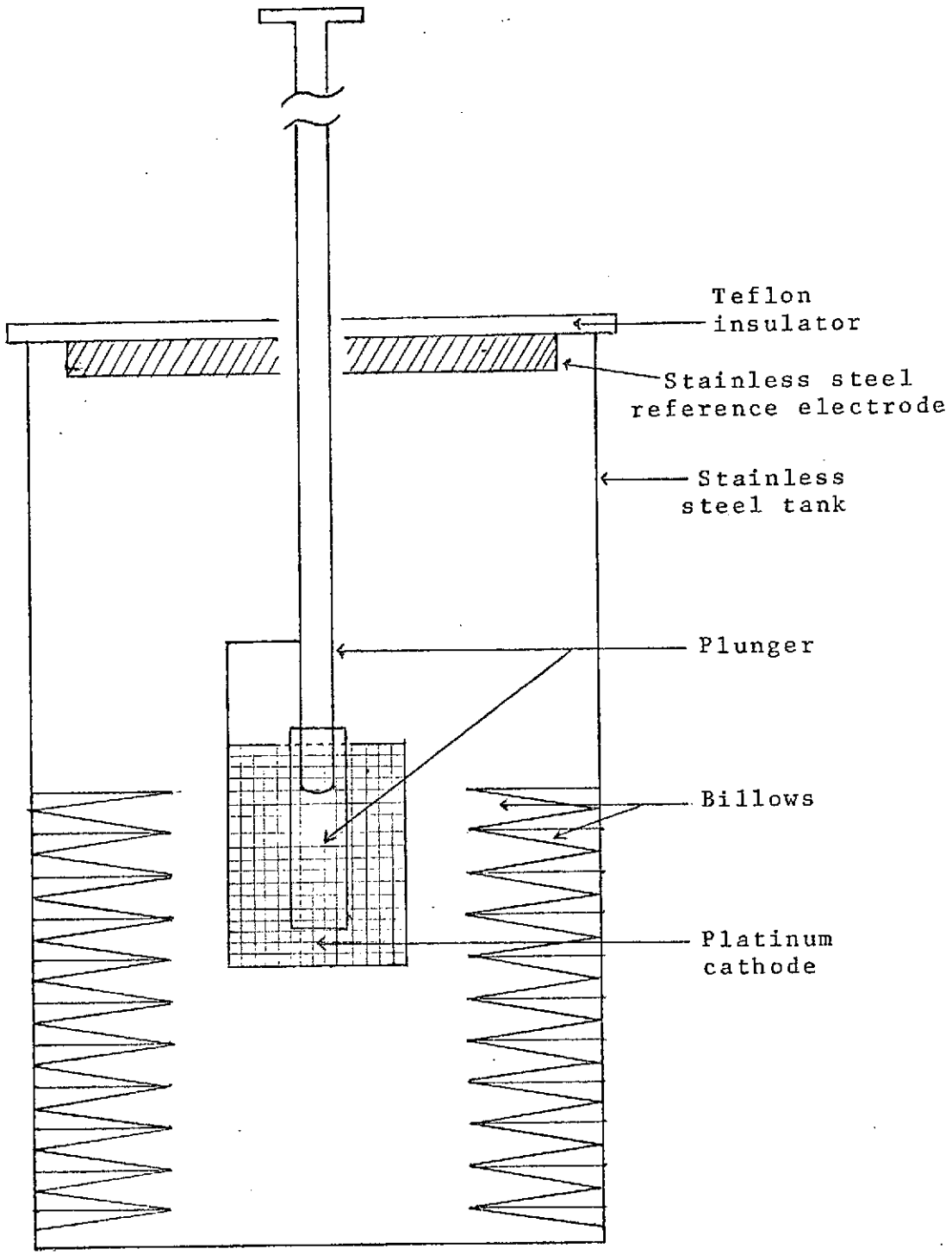
Teflon
insulator
Stainless steel
reference electrode
Stainless
steel tank
Plunger
Billows
Platinum
cathode

Fig. 26.

Figure 27.

Iodine production rates on the simulated Skylab tank in distilled water containing 50 ppm KI. Room conditions. Surface area was approximately 75 cm^2.

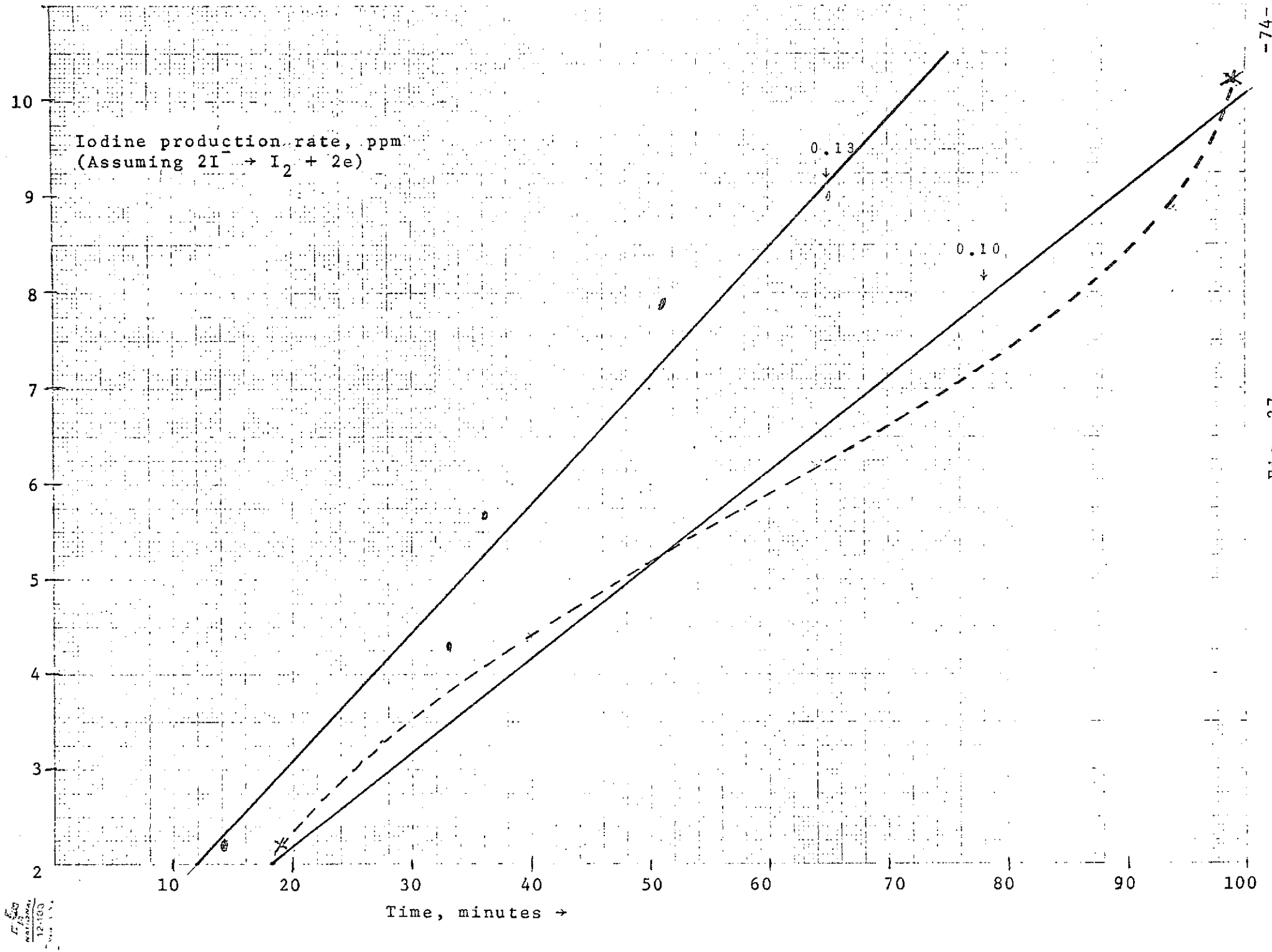

Fig. 27

At +1000 mv vs. SCE the iodine production rate from distilled water containing 500 ppm KI (382 ppm I^-) was 0.49 ppm/cm^2/min. compared with approximately 0.0017 and 0.0013 ppm/cm^2/min for the simulated tank at +1000 mv vs. stainless steel. Some of this decrease in production rate was due to the former solution being an order of magnitude more concentrated. The decrease in production rate may also be due in part to anodic dissolution of the stainless steel.

It was also observed that the solution color after anodic polarization was more cloudy than in previous iodine production studies. A careful visual examination revealed that a reddish solid material was suspended in the liquid. After four and one-half hours in a solution of 50 ppm KI in distilled water, with the tank at open circuit (no external polarization) showed iron and chromium concentrations in solution of 0.1 and 0.005 ppm respectively. No reddish color was present. After polarization at +1000 mv for 112 minutes, the iron and chromium concentrations increased to 0.6 and 0.3 ppm respectively. However, the reddish solid was found to be present. When the reddish solid was dissolved in acid, the iron and chromium concentrations were found to increase to 6.5 and 1.0 ppm respectively. The stainless steel tank was therefore dissolving under anodic polarization. This disadvantage may be attributed to the low anodic current density which necessitates large anodic potentials so that a

measurable iodine production rate may be obtained.

Another possible explanation of these high ion contents in the geometry of the "tank" or electrochemical cell configuration. The anode is very large compared to the cathode, which means that the anodic current density (iodine production) is low and cathodic current density (hydrogen production) is high. As hydrogen is evolved ($2H_2O + 2e \quad H_2 + 2OH^-$), the solution becomes slightly basic. In the more basic solution, the stainless steel dissolves to give the reddish iron-hydroxide precipitate or complex.

If the stainless steel tanks are used as anodes, a method must be used to greatly increase the surface area of the cathode. Another possibility is to use the stainless steel tank as the cathode and a smaller stainless steel or platinum electrode as the anode. This would provide the advantage of having some cathodic protection to the stainless steel tank, plus decrease the cathodic current density (hydrogen evolution). The anode size could then be selected to provide a high anodic current density for iodine production. In 3.6N H_2SO_4 the oxide film on stainless steel was reduced near -400 mv vs. SCE. In essentially neutral solutions, as anticipated for the Skylab system, this reduction is not expected; however, dissolution rates over long periods of time

for the stainless steel under reducing conditions should be measured in order to demonstrate this phenomenon.

Future Work

1. Measure the loss of I^-, I_2 or I_3^- with time from dilute solutions.
2. Measure stainless steel dissolution rates under various conditions, including reducing conditions.
3. Study teflon film (or other materials) as diaphrams between the anode and cathode.
4. Study the cathode behavior of the stainless steel tank.
5. Demonstrate a working model of the proposed electrochemical system.